LOW FREQUENCY HYDROMAGNETIC WAVES IN THE MAGNETOSPHERE

by

Vithalbhai L. Patel

Physics Department
University of New Hampshire
Durham, New Hampshire

A dissertation submitted in partial fulfillment of the requirements for the degree of Doctor of Philosophy

June 1964

*Supported by the National Aeronautics and Space Administration under Contract NASw-155.

This thesis has been examined and approved.

_____

_____

_____

_____

_____

_____

Date

ACKNOWLEDGEMENT

The author wishes to express his sincere gratitude to Professor L. J. Cahill, Jr. for his guidance and advice not only during this research, but throughout the association with him. His direction in this research has made this work possible and complete. The author also wishes to thank the faculty research committee for their critical reading and suggestions.

The author is thankful to Dr. M. Sugiura, Goddard Space Flight Center, Greenbelt, Maryland for his help and correspondence regarding the work in Chapter IV. The computational work was carried out at Goddard Space Flight Center and the University of New Hampshire Computation Center. The author wishes to thank members of the data reduction group for their assistance. He is also thankful to H. Caulk and Mrs. Marilyn Wingersky for assistance in programming.

The author wishes to thank his wife Pushpa Patel for computational help, typing and patience, and to Sandra Noel for typing and assembly of the thesis.

The author wishes to express his indebtedness to the trustees of R. H. Patuck Education Trust Foundation, Bombay for an award which made his travel to the U. S. A. possible.

This research was supported by National Aeronautics and Space Administration Contract NASw-155.

TABLE OF CONTENTS

LIST OF TABLES

LIST OF FIGURES

CHAPTER I

INTRODUCTION

1. General

The study of the origin and propagation of electromagnetic waves is one of the oldest problems considered by physicists and mathematicians. The first part of the spectrum of the electromagnetic waves studied was the "visible light" region. This was of more interest to study because of the fact that it affected human sensory organs. Other parts of the spectrum studied well were the "ultraviolet", "infrared", and "radio frequency" regions. The advent of modern physics and technology extended our knowledge to the far end of the spectrum on the side of very small wave lengths, e.g. X rays of wave length 10^{-9} to 10^{-10} meter and gamma rays 10^{-10} to 10^{-14} meter. Also low frequency "radio" waves with frequencies of a few kilocycles per second have been studied. Every part of the electromagnetic spectrum has helped us to learn more about the physical world, e.g., wave lengths of 10^{-7} to 10^{-14}m gave insight into atomic and nuclear phenomena, while the well known 21 cm wave length radiation from the clouds of interstellar hydrogen gave information about the galaxy. Frequencies of a few kilocycles per second constitute the ' probe' that can tell us about the earth's magnetosphere (region of space dominated by the earth's magnetic field) as far as 3 to 5 earth radii (R_E).

These waves of 10^6m wave length (so called "Whistlers") are very useful for the study of the electron density in the magnetosphere. However, the far low frequency end of the spectrum remained unexplored, i.e., the region of very long wave length and very small frequencies. In Figure 1 which scans the whole range of the spectrum, the region under discussion is of wave lengths 10^9 to 10^{11} meters (frequencies of 1 to 10^{-3} cps). It is known that low frequency electromagnetic waves in the presence of a magnetic field and a plasma become waves of a different type called "Alfven" waves or hydromagnetic waves. Our primary interest is to study such low frequency hydromagnetic waves. It will be shown that the production of such waves requires special conditions which are not easily obtained in the laboratory.

This was one of the reasons that interest in the area of the low frequency waves only recently developed. It was in 1942 that these waves were postulated by Alfven[1]. The method of detection of these waves is different from the conventional methods. Instead of the electric component of the waves, the magnetic component is more easily detected. The amplitude of the magnetic component of these waves is so small that very sensitive magnetometers are required. Preliminary studies were done as early as 1920 (Angenheister and Rolf) to detect small changes in the earth's magnetic field. These investigations were only observational studies, however, and it was not understood that the small regular changes in the earth's field might be hydromagnetic waves transformed into electromagnetic waves in the lower

ionosphere. The reason again was our lack of awareness of "hydromagnetic" phenomena at that time.

In 1954, Dungey attempted in a very careful manner a theoretical study of oscillatory variations of the earth's field[2]. His work was so intensive that it induced many other workers to work on details of these problems. He tried to identify the frequencies of oscillation of the earth's field as eigenperiods of the oscillatory outer atmosphere. This involved many assumptions and simplifications in the problem. The important contribution was to consider the small variations in the earth's magnetic field (micropulsations) as a manifestation of hydromagnetic waves originated somewhere in the earth's outer atmosphere (Dungey assumed the boundary of the geomagnetic field at 10 to 12 R_E as the source of the disturbance) and propagated downward to the earth. Sugiura[3] presented the first observational evidence of hydromagnetic waves found in ground magnetometer records. This work is related to our study and will be discussed in detail in Chapter II.

As mentioned before, the hydromagnetic wave changes into an electromagnetic wave in the lower ionosphere and the magnetic component of this wave is the cause of "micropulsations". Realization of this opened a new field of investigation, since geophysical dimensions are appropriate for the generation of low frequency hydromagnetic waves. The problem is not simple, and since the "micropulsations" are complex phenomena. Systematic studies of long period micropulsations has been difficult since it is complicated

by the fact that so many simultaneous disturbances are involved. Information on the particle density and temperature in the outer atmosphere, pertinent to wave propagation, has not been available. This situation has been somewhat remedied by the use of artificial satellites in recent years.

2. Statement of the Problem

It is our intention to learn more about these complex phenomena by using the magnetic field measurements in space obtained by the artificial earth satellite Explorer XII. The low frequency hydromagnetic waves serve as a probe of the more distant ($5-10\ R_E$) regions of the magnetosphere[4]. The most effective way to learn as much as we can about the low frequency hydromagnetic waves is to investigate them in space by using satellite measurements of the magnetic field, and simultaneously identifying them in ground magnetometer records. It is the primary aim of this investigation to study the frequencies, amplitudes, polarizations and modes of propagation of the low frequency hydromagnetic waves existing in the magnetosphere of the earth at equatorial distances between 5 to 10 R_E and to identify them with changes in the earth's magnetic field at the ground level.

Before going to this problem, we shall review the concepts in "magnetohydrodynamics" pertinent to our problem and recent theoretical work on hydromagnetic waves. On the experimental side, an account of the magnetometers employed in the Explorer 12 experiment will be given.

3. Basic Principle of Magnetohydrodynamics

The subject of magnetohydrodynamics or hydromagnetics was put on the firm basis by Alfven in 1942. Speculations about this phenomenon really started as early as 1908 when Hale discovered that the sun has a magnetic field. His discovery opened discussion on the theory of sunspots. Cowling suggested the idea of a convection of magnetic field from deep layers of the sun to its surface. However, the concept of a "frozen-in" field was not well understood.

Alfven[5] clearly stated for the first time the theorem that in a highly conducting fluid embedded in a magnetic field relative motion between the matter and the field lines is prohibited. His theorem is as follows:

> "Every motion (perpendicular to the field) of the liquid in relation to the lines of force is forbidden because it can give infinite eddy currents. The matter of the liquid is fastened to the lines of force."

The mathematical proof if very simple[6]. Consider the Maxwell equation from Farady's induction law,

$$\nabla \times \underline{E} = -\frac{\partial \underline{B}}{\partial t} \tag{3.1}$$

and Ohm's law,

$$\underline{J} = \sigma\left(\underline{E} + \underline{v} \times \underline{B}\right) \tag{3.2}$$

where σ is the conductivity and $\underline{v}$ the velocity of the fluid which has magnetic induction B in it. (The validity of (3.2) will be justified in Appendix A) Now if $\sigma \to \infty$, we obtain,

$$\underline{E} = -\underline{v} \times \underline{B} \tag{3.3}$$

This means that there is no electric field in the system moving with the fluid velocity $\underline{v}$. Using this value of $\underline{E}$ from equation (3.3) in (3.1) we get

$$\nabla \times (\underline{v} \times \underline{B}) = \frac{\partial \underline{B}}{\partial t} \tag{3.4}$$

This implies that the flux of magnetic induction through a circuit of fluid particles is constant. The above condition is illustrated by considering a surface S bounded by the a closed curve C made up of the particles.

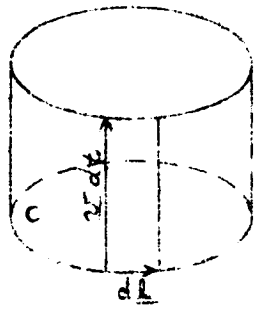

The magnetic flux ϕ_m through surface S is

$$\phi_m = \iint_S \underline{B} \cdot d\underline{s} \tag{3.5}$$

As the surface S and curve C move, the change in ϕ_m consists of a local change $\frac{\partial \phi_m}{\partial t}$ and the change due to the motion of a curve C which is given by considering that an element of curve $\underline{dl}$ moves $\underline{v}\,dt$ in time dt and sweeps area

$$(\underline{dl} \times \underline{v})\,dt. \tag{3.6}$$

The flux through this surface element is

$$\underline{B} \cdot (\underline{dl} \times \underline{v})\,dt \tag{3.7}$$

and its rate of change is

$$\underline{B} \cdot (\underline{dl} \times \underline{v}) = \underline{v} \times \underline{B} \cdot \underline{dl}.$$

Integration around C gives the rate of decrease of flux through area S due to the motion of C,

$$\therefore \frac{d\phi_m}{dt} = \frac{\partial \phi_m}{\partial t} - \oint_C (\underline{v} \times \underline{B}) \cdot d\underline{l} \qquad (3.8)$$

By Stoke's theorem and using equation (3.5)

$$\frac{d\phi_m}{dt} = \iint_S \left\{ \frac{\partial \underline{B}}{\partial t} - \nabla \times (\underline{v} \times \underline{B}) \right\} \cdot d\underline{\Sigma} \, . \qquad (3.9)$$

By equation (3.4) the right hand side equals to zero. Therefore

$$\phi_m = \text{Constant} \qquad (3.10)$$

This is a very important conclusion. It implies that there may be motion of the fluid along the lines of force of the magnetic field, but that any motion perpendicular to the lines of force carries them with the fluid. This law, therefore opened a new branch of cosmical physics, magneto-hydrodynamics.

Now let us consider the conditions that we used to achieve these results. The only condition used here is that the fluid is highly conducting, i.e., $\sigma \to \infty$. However, this condition alone is not enough to observe "hydromagnetic" phenomena. For this reason we shall consider the fundamental equations of magnetohydrodynamics and carefully note the approximations made in this process. We shall show that in addition to the condition $\sigma \to \infty$, conditions on characteristic length and time must be satisfied to observe the phenomenon. Usually large dimensions are necessary to satisfy these conditions. We shall bring out the

difference in the approach of laboratory electrodynamics and cosmical electrodynamics (by cosmical, we mean large dimensions compared to laboratory dimensions) including the reason that laboratory experiments did not reveal these effects. In later sections we shall show that all these conditions are satisfied in the region of the magnetosphere in which we are interested.

4. Fundamental Equations and Approximations in Hydromagnetics

Before 1942, the motion of ions in electromagnetic fields was considered by taking into account the action of the field on the ions. The action of ions on the fields was neglected. Alfven[1] considered the mutual interplay of the action of the fields on the ions and action of the ions on the fields.

To make the situation more clear, let us consider a conducting fluid moving with velocity $\underline{v}$ in the magnetic field $\underline{B}$. This motion induces an electric field $\underline{v} \times \underline{B}$, which sets up currents and further modifies the original $\underline{B}$ field exerting pressure on the fluid. These processes are best depicted in Figure 3 and are given mathematically by the following equations. These are combinations of Maxwell's equations and hydrodynamic equations.

$$\underline{E}' = \underline{E} + \underline{v} \times \underline{B} \tag{4.1}$$

$$\underline{J} = \sigma \underline{E}' \tag{4.2}$$

$$\nabla \times \underline{H} = \underline{J} \tag{4.3}$$

$$\nabla \times \underline{E} = -\frac{\partial \underline{B}}{\partial t} \tag{4.4}$$

$$\nabla \cdot \underline{E} = \rho/\epsilon_0 \tag{4.5}$$

$$\underline{F_e} = \underline{J} \times \underline{B} \tag{4.6}$$

$$\frac{d\underline{v}}{dt} \cdot f_m = \underline{F_e} + \underline{F_o} \tag{4.7}$$

$$\frac{\partial \rho_m}{\partial t} + \nabla \cdot (\rho_m \cdot \underline{v}) = 0 \tag{4.8}$$

In the above equations, f_m is the density of matter, ρ the density of charge, $\underline{F_e}$ the electromagnetic force, $\underline{F_o}$ force due to the gradient of pressure etc., and other symbols have the usual meaning.

Let us examine the above equations one by one and consider them carefully in the light of their physical significance and the approximations made in their use. Equation (4.1) gives $\underline{E}$ in the reference frame moving with the fluid. The term $\underline{v} \times \underline{B}$ is due to the induction field and $\underline{E}$ is obtained from equation (4.4) and not from the space charge equation (4.5). This is the difference between laboratory electrodynamics and cosmic electrodynamics which will be discussed in more detail in the next section. At present, the above explanation will suffice.

Equation (4.2) needs very careful examination. It is the familiar Ohm's law and its validity can be questioned in the problems with which we shall be concerned. We are interested in the hydromagnetic problems in the mag-

netosphere covering the geocentric distance 5 to 10 R_E. Considering the fully ionized plasma there, it is shown in Appendix A (also see Spitzer, Ginzburg, or any standard book on plasma physics) that equation (4.2) holds if

$$\omega << \Omega_i \tag{4.9}$$

$$\omega << \nu_{ei} \tag{4.10}$$

$$\omega_e << \nu_{ei} \tag{4.11}$$

where ω is the frequency of changes in magnetic field, Ω_i is Larmor ion frequency, ω_e is the Larmor electron frequency and ν_{ei} is the electron-ion collision frequency. These conditions allow us to neglect ∇p_e, $\underline{J} \times \underline{B}$, and $\frac{\partial \underline{J}}{\partial t}$ terms in the generalized Ohm's law which leads to equation (4.2). Actually this relation is the "hydromagnetic" condition in the sense that it tells us that the ionized gas can be treated as a fluid*. This relation is easy to satisfy in astrophysical and certain geophysical problems. Following Figure 3, the currents set up affect the magnetic field, from which we get equation (4.3). This equation needs further consideration. The total current $\underline{J}$ flowing in the medium is made of three parts:

---

*In fact, the condition $\omega << \omega_e$ is not satisfied as can be seen in Appendix B, but the condition for using the hydrodynamic description is fulfilled by the condition $\omega << \Omega_i$. This condition is sufficient but not necessary, the necessary condition is $\omega << (\Omega_i^2 + \nu_{ei}^2)^{1/2}$. Both of these conditions are well satisfied in the magnetosphere (see Appendix B) and the plasma there can be considered as fluid.

$$J_{Total} = J_{conv} + J_{cond} + J_{disp} \qquad (4.12)$$

The convection current is negligible if $v \ll C$ and the displacement current is negligible for low frequency waves[13]. Since J_{conv} and J_{disp} can be neglected compared to J_{cond} in the problems in which we are interested, the equation takes the form

$$\nabla \times \underline{H} = \underline{J}_{conv} = \underline{J} \qquad (4.3)$$

The above approximation of neglecting displacement current raises a further question if we consider the interpretation of Maxwell's introduction of displacement current. This current was introduced to make $\underline{J}$ solenoidal, i.e.,

$$\nabla \cdot \underline{J} = 0$$

Physically, this means that discontinuities in the current due to accumulation of charges at points are neglected. The current then flows in a closed circuit. The neglect of the displacement current implies that interruption of current flow due to a space charge should be neglected, i.e., the currents which cause space charge at boundaries should be neglected. Therefore, $\nabla \cdot J_{cond} = 0$ and we can neglect the force term $\underline{E}$ due to space charge in the equation of motion. The space charge itself is not neglected. In fact the space charge plays important roles in many problems.

Therefore, we shall not use $\nabla \cdot \underline{E} = \frac{\rho}{\epsilon}$ further in magnetohydrodynamics, but we cannot write $\nabla \cdot \underline{E} = 0$ either. Instead it is approximated as $\nabla \cdot \underline{E} = \frac{E}{L_c}$ where L_c is the

dimension of the system.

The approximations considered in this section are:

1) Ohm's law holds in the form $\underline{J} = \sigma \underline{E}$.
2) Displacement and convection currents are neglected.

5. Condition for "Frozen-in" Fields

In Section 3, we showed with the approximation $\sigma \to \infty$ that there cannot be relative motion between matter and the magnetic field (in the perpendicular direction) in a highly conducting fluid. However, we did not consider the actual physical conditions for which this can be realized, i.e. the dimensions of the system and the time constant. In order to get some idea about these quantities consider the equations (4.1), (4.2), (4.3) and (4.4) without considering $\sigma \to \infty$ then, we get

$$\nabla^2 \underline{H} = \sigma\mu \left\{ \frac{\partial \underline{H}}{\partial t} - \nabla \times (\underline{v} \times \underline{H}) \right\} \tag{5.1}$$

Consider two cases in the above equation.

(a) Assume $\underline{v} = 0$, we have the diffusion equation

$$\nabla^2 \underline{H} = \frac{1}{\eta} \frac{\partial \underline{H}}{\partial t} \quad ; \quad \eta = \frac{1}{\sigma\mu} \tag{5.2}$$

This diffusion equation has a time constant

$$t_D = \mu\sigma L^2 \tag{5.3}$$

where L is the linear dimension. It means that the field decreases by 1/e due to "slipping" or "leakage" through the conductor, in a time t_D when the system is stationary.

Some examples of this are[7]:

1. Copper sphere of 1 m diameter has $t_D \sim 10$ sec.
2. Earth's field has a decay time $t_D \sim 15000$ years.
3. Sunspot has decay time of 300 years.
4. Mercury sample in the laboratory has a decay time of less than one second.

These examples show that long time constants are possible in astrophysical and geophysical phenomena, but laboratory conditions lead to smaller time constants.

(b) Now consider $\sigma \to \infty$

$$\frac{\partial \underline{H}}{\partial t} = \nabla \times (\underline{v} \times \underline{H}) \tag{5.4}$$

This also means that $\nabla \times \underline{E}' = 0$. Any $\underline{E}'$ field in the plasma cloud is curl free and the magnetic field is "frozen-in" as shown in Section 3.

When both (a) and (b) hold, i.e., when a highly conducting medium is in motion, which is a frequent case in geophysical problems, we can get a condition by which the diffusion would be negligible. If the motion is completed in a time very small compared with the time constant t_D, the diffusion is negligible and convection predominates. That is, if

$$\frac{L}{v} << t_L = \mu \sigma L^2 \tag{5.5}$$

we have

$$\mu \sigma L v >> 1$$

This condition implies that $\sigma \to \infty$ alone is not enough to observe hydromagnetic effects. The dimension of the system also should be very large.

The lines of magnetic force leak very slowly through the conductor in a very large conducting mass. However, it is understood that magnetic field should be large enough (at least $\frac{B^2}{\mu} \simeq \rho v^2$) for the effective coupling of electromagnetic and material forces. Because of the required large dimensions to satisfy condition (5.5), "hydromagnetics" was not discovered for a long time. Some experiments in the laboratory were performed by Lundquist[8] with mercury and sodium following Alfven's work and more recently by Wilcox with plasma[9]. These experiments confirmed the prediction of Alfven. But many times, laboratory experiments may be misleading because of the limitations on space and time scales. Recently solid state plasma studies have been used successfully with electronic techniques to study Alfven waves.

Whatever precautions may be taken in the laboratory, only a very crude picture of cosmic phenomena can be reproduced. Therefore, we can only get a glimpse of cosmic phenomena in the laboratory. In Section 6, the fundamental difference in the approach to cosmic electrodynamics will be considered. One clear difference can be seen from the equation (5.1) of this section. Rewrite this equation as

$$\frac{\partial \underline{H}}{\partial t} = \nabla \times (\underline{v} \times \underline{H}) + \eta \nabla^2 \underline{H} \qquad (5.6)$$

We know that the currents in a laboratory conductor are mainly determined by conductivity σ. But σ has very little immediate effect on the current in the cosmic case. A large change in σ will produce no great change in $\underline{H}$ and

so no change in the current. It will affect only the second term in equation (5.6) which itself is very small compared to the first term. A discussion of cosmical electrodynamics which leads to the existence of Alfven waves, will be the topic for the following section.

6. Cosmical Electrodynamics

Let us first consider ordinary laboratory electrodynamics. We shall ask such questions as: "What drives the current? Where does the electric field come from?" The answer is that the current is driven by the electric field and the electric field is produced by the space charge and the change in the magnetic field. We can represent the scheme as follows:

$$\frac{\partial \underline{B}}{\partial t} \longrightarrow \underline{E} \overset{\rho}{\longrightarrow} \underline{J} \overset{\underline{v}}{\longrightarrow} \underline{B}$$

This familiar approach to electrodynamics is inappropriate to cosmic electrodynamics. Another approach is given by Cowling[10] and Dungey[11] in which the above order is, in fact, reversed.

In Section 4 we have argued that space charge is of little interest in the cosmic electrodynamics. Therefore, the approach taken is that we do not calculate fields from the sources, but calculate the sources from the given fields. This approach reverses the above order of the cause and effect. This new scheme will be deduced from the basic equations which satisfy the initial values of certain quantities. Then we compute their values after a certain time.

We should select the equation that is appropriate and if it contains a time derivative, it determines that time derivative and other equations determine other variables in a unique way. Let us consider these basic equations of cosmical electrodynamics the use of which we have already justified.

7. Basic Equations of Cosmic Electrodynamics

(1) Maxwell's equations in the following forms:

$$\nabla \times \underline{H} = \underline{J} \tag{7.1}$$

$$\nabla \times \underline{E} = -\frac{\partial \underline{E}}{\partial t} \tag{7.2}$$

(2) A form of Ohm's law which is

$$\frac{m_e}{ne^2}\frac{\partial \underline{J}}{\partial t} = \underline{E} + \underline{v} \times \underline{B} - \frac{\underline{J}}{\sigma} \tag{7.3}$$

and reduces to

$$\underline{E} + \underline{v} \times \underline{B} = 0 \tag{3.3}$$

(3) Equations of transfer of momentum

(4) Equations of conservation of mass

Now applying our method for any problem in which initial values are given we have from (7.1) and (7.2)

$$\underline{B} \longrightarrow \underline{J}$$

$$\underline{E} \longrightarrow \underline{B}$$

Further, equation (7.3) determines $\underline{E}$, if we consider that $\frac{\partial \underline{J}}{\partial t}$ and $\underline{v} = 0$. The scheme is

$$\underline{E} \longrightarrow \underline{B}$$
$$\uparrow \quad \swarrow$$
$$\underline{J}$$

But most cosmical problems involve motion and we can rewrite the above scheme as follows:

$$\begin{array}{ccc} \underline{v} & \longrightarrow & \underline{E} \\ \uparrow & & \downarrow \\ \underline{J} & \longleftarrow & \underline{B} \end{array}$$

This scheme is just in the reverse order of the usual laboratory one. Therefore, the questions asked in the case of laboratory electrodynamics have no meaning in cosmic electrodynamics. If we eliminate $\underline{E}$ by equation (3.3) and $\underline{J}$ by equation (7.1) we get from the above scheme.

$$\underline{v} \longleftrightarrow \underline{B}$$

The above result is equivalent to Alfven's approach[12]. When Alfven elucidated the "frozen-in" field concept, he ingeniously predicted that disturbances in a highly conducting fluid permeated by a magnetic field could be transmitted without mass motion of the fluid. Under ordinary conditions, this is possible only by mass motion. He restricted his discussion to the case of transverse waves travelling along the lines of force.

In the next section, we want to study these waves in a compressible fluid in greater detail and then study them, in other chapters, on the geophysical scale in the magnetosphere of the earth.

CHAPTER II

LOW FREQUENCY HYDROMAGNETIC WAVES IN A HOMOGENEOUS MAGNETOACTIVE PLASMA

1. The Hydromagnetic Approximation in Plasmadynamics

In order to study the motion in a plasma, we should consider the field equations and kinetic equations of electrons, ions and neutral molecules. This is so complicated, that in practice various approximation methods are used for the solutions of dynamic problems in a plasma. The approximations used are:

a) Equilibrium Theory: Maxwell's distribution function is used to calculate kinetic and transport properties. This is used assuming that the plasma is in equalibrium.

b) Orbit Theory: The motion of the particles is described in the electric field and magnetic field. The approximation is good when the collisions are not important, i.e., when the mean free path is large compared with the characteristic length. This approximation is equivalent to the Boltzmann equation in the absence of collisions.

c) Hydromagnetic Approximations: The description of the gas is done by means of the equations of hydrodynamics. This approximation is most

important here and will be used in discussing the propagation of the waves in the plasma. The conditions in which this approximation can be applied are discussed in Chapter I.

The complete and systematic conditions of the hydromagnetic approximations will now be given.

$$l \ll L_c \tag{1.1}$$

where l is the mean free path and L_c is the characteristic length in the problem, e.g., wave lengths or dimensions of containers.

Also,

$$\tau_{eff} = \frac{1}{\nu_{eff}} = \frac{l}{v_T} \ll t_c \sim \frac{2\pi}{\omega} \tag{1.2}$$

where τ_{eff} is the time of free flight and $v_T = \left(\frac{kT}{m_i}\right)^{1/2}$ and t_c is the characteristic time such as the period of oscillation. Another condition is

$$T_i \ll t_c \tag{1.3}$$

where T_i is the ion Larmor period and is given by

$$T_i = \frac{2\pi m_i c}{eB} = \frac{2\pi}{\Omega_i}$$

We can write these last two conditions as

$$\omega \ll \nu_{eff} \tag{1.4}$$

$$\omega \ll \Omega_i \tag{1.5}$$

The condition (1.4) automatically satisfies condition (1.1), i.e., $l \ll L_c$ for the macroscopic motion $\nu \ll v_T$. The other condition is

$$\omega_e << \nu_{eff} \tag{1.6}$$

where $\omega_e = \frac{eB}{m_e}$. However, Ohm's law for a fully ionized plasma gives conditions (1.4), (1.5) and (1.6) as shown in Appendix A.

Actually, the above conditions are physically equivalent to saying that the medium becomes isotropic even in the presence of a magnetic field in the frame of coordinates where its velocity is zero. (It can be seen that condition (1.6) makes the conductivity isotropic[13].)

With these conditions in mind, low frequency wave propagation in the plasma can be studied. However, conditions (1.4) and (1.6) are not satisfied in most problems, particularly when collisions are neglected. When the approximation inequalities (1.4) and (1.6) are not satisfied, the quasi-hydromagnetic approximation may be employed. The quasi-hydromagnetic approximation utilizes average quantities along with the use of a distribution function[14]. It may be shown that hydromagnetic waves are possible even when $\nu_{eff} \approx C$; when hydromagnetic approximation may not hold. In the case of rarefied plasmas, condition (1.6) may fail, but the equations for hydromagnetic waves are still valid. In Appendix B it is shown by numerical values that all other conditions are satisfied for the low frequency magnetohydrodynamics waves in the earth's magnetosphere, which is the subject of study in Chapter IV. In the next section low frequency hydromagnetic waves in a

plasma are considered in detail.

2. Alfven and Magneto-acoustic Waves in a Compressible Plasma

We shall study the magnetohydrodynamic waves of various types in a plasma with uniform magnetic field. Banos[15] has shown that as many as six kinds of waves are possible in a plasma, but we shall be concerned with only three which occur most frequently and are simple to discuss.

We assume that hydromagnetic conditions (1.4) and (1.6) in Section 1 of this Chapter and other conditions discussed in Chapter I are satisfied. The condition (1.6) is not satisfied in the magnetosphere. Modification due to this fact will be made later on. We disregard viscosity and thermal conductivity and assume that $\sigma \to \infty$. The plasma is regarded as a uniform and compressible medium and a uniform magnetic field is present. The following treatment is valid when $\nu_{eff} \simeq 0$. The plasma may be highly rarefied, $\nu_{eff} = 0$, and therefore this treatment is quite general in nature. There are, however, limits on the frequency of the waves. Our previous discussion on the approximations of magnetohydrodynamics (Chapter I, Section 4) implies that $\omega \ll \omega_i$. This means that the waves we shall discuss by magnetohydrodynamic approximation are "low frequency" waves. This restriction ensures that the ions and electrons are "frozen-in" to the magnetic lines of force and one need not take into consideration the relative motion between the particles and the field lines. Stringer[16] has considered waves

of low frequencies in all ranges in a general way.

With the above approximation Alfven first saw from an intuitive point of view that since the material is frozen to the field lines this is equivalent to considering the lines as material strings. The vibration of the material string can be written as

$$T \frac{\partial^2 b}{\partial x^2} = \rho_m \frac{\partial^2 b}{\partial t^2} \tag{2.1}$$

where B_o is along the X axis and $\underline{B} = \underline{B}_o + \underline{b}$. T represents the tension and ρ_m is the density of the matter. The tension here is

$$T = \frac{B_o^2}{\mu} \tag{2.2}$$

Therefore,

$$\frac{\partial^2 b}{\partial t^2} = \frac{B_o^2}{\mu \rho_m} \frac{\partial^2 b}{\partial x^2} \tag{2.3}$$

with a velocity of propagation $U_A = \frac{B_o}{\sqrt{\mu \rho_m}}$. These, Alfven waves, are transverse waves in the incompressible fluid[1]. It is shown in Appendix C that these waves are electromagnetic waves propagating in a plasma with magnetic field in the low frequency limit.

Now consider, with all the assumptions mentioned above, a compressible, isotropic conducting medium. (The anisotropic medium will be considered in Chapter III). It will be seen that longitudinal waves may be excited in this case. The low frequency approximation allows us to use equation (3.3) of Chapter I; other basic equations are:

$$\nabla \cdot \underline{B} = 0 \tag{2.4}$$

$$\frac{\partial \underline{B}}{\partial t} = \nabla \times (\underline{v} \times \underline{B}) \tag{2.5}$$

$$\frac{\partial \rho}{\partial t} + \nabla \cdot (\rho \underline{v}) = 0 \tag{2.6}$$

$$\rho \frac{d\underline{v}}{dt} = \rho \left\{ \frac{\partial \underline{v}}{\partial t} + (\underline{v} \cdot \nabla) \underline{v} \right\} = -\nabla p + \frac{1}{\mu} (\nabla \times \underline{B}) \times \underline{B} \tag{2.7}$$

$$\rho = \rho_{...} \quad ; \quad \underline{B} = \mu \underline{H} \tag{2.8}$$

Considering waves of small amplitudes, we assume that the departures from equilibrium are small.

$$\underline{B} = \underline{B}_0 + \underline{b} \tag{2.9}$$

$$\rho = \rho_0 + \rho' \tag{2.10}$$

$$p = p_0 + p' \tag{2.11}$$

$$\underline{v} = 0 + \underline{v}' \tag{2.12}$$

where p is the gas pressure. For an adiabatic approximation (in absence of dissipation)

$$\frac{\delta p}{p} = \gamma \frac{\delta \rho}{\rho} \tag{2.13}$$

$$p' = \delta p = \gamma \frac{\delta \rho}{\rho} p = U_s^2 \delta \rho = U_s^2 \rho' \tag{2.14}$$

where U_s is the velocity of sound in the gas.

Using the above equations in equations (2.4) through (2.7) and neglecting higher order terms we get

$$\nabla \cdot \underline{b} = 0 \tag{2.15}$$

$$\frac{\partial \underline{b}}{\partial t} = \nabla \times (\underline{v} \times \underline{B}) \tag{2.16}$$

$$\frac{\partial \rho'}{\partial t} + \rho \nabla \cdot \underline{v} = 0 \tag{2.17}$$

$$\frac{\partial \underline{v}}{\partial t} = -\frac{U_s^2}{\rho_o} \nabla \rho' + \frac{1}{\rho_o \mu} (\nabla \times \underline{b}) \times \underline{B} \qquad (2.18)$$

Omitting the subscript o in the above equations, we seek a solution of the form

$$e^{i(\underline{k}\cdot\underline{r} - \omega t)}$$

This describes a plane wave with wave vector $\underline{k}$ and frequency ω. Suppose that $\underline{k}$ is along the X-axis, B_o lies in the (x, y) plane and makes an angle θ with X axis, i.e., $B_o = (B_o \cos\theta, B_o \sin\theta, o)$. Substituting $e^{i(\underline{k}\cdot\underline{r} - \omega t)}$, we get the equations,

$$-\omega \underline{b} = \underline{k} \times (\underline{v} \times \underline{B}) \qquad (2.19)$$

$$\omega \rho' = \rho \, \underline{k} \cdot \underline{v} \qquad (2.20)$$

$$-\omega \underline{v} + \left(\frac{U_s^2}{\rho}\right) \rho' \underline{k} = -\frac{1}{\mu \rho} \left\{ \underline{B} \times (\underline{k} \times \underline{b}) \right\} \qquad (2.21)$$

Eliminating ρ' and using the phase velocity $U = \frac{\omega}{k}$, the components separate into the equations

$$U b_z = -v_z b_x \quad ; \quad U v_z = -\frac{B_x b_z}{\mu \rho} \qquad (2.22)$$

$$U b_y = v_x B_y - v_y B_x \quad ; \quad U v_y = -\frac{B_x b_y}{\mu \rho}$$

$$v_x \left(U - \frac{U_s^2}{U}\right) = \frac{B_y b_y}{\mu \rho} \qquad (2.23)$$

These equations form two groups, one involving $\underline{b}$ and $\underline{v}$ and another involving, b_y, v_x, v_y. From these equations we shall find three types of the waves. The first and most familiar one is obtained by eliminating v_z from

equations (2.22). Such a wave is called an Alfven or hydromagnetic wave; its phase velocity is given by

$$U_1 = U_x = \frac{B_x}{\sqrt{\mu\rho}} \tag{2.24}$$

The dispersion relation for this wave is

$$\omega = \frac{\underline{B}\cdot\underline{k}}{\sqrt{\mu\rho}}$$

The group velocity is, therefore

$$U_{1g} = \frac{\partial\omega}{\partial\underline{k}} = \frac{\underline{B}}{\sqrt{\mu\rho}} = U_A \tag{2.25}$$

This wave is the Alfven wave which was discussed previously. In these waves, the component b_z is perpendicular to $\underline{k}$ and $\underline{B}$ and has the velocity

$$v_z = -\frac{b_z}{\sqrt{\mu\rho}}$$

(1) For longitudinal propagation $\theta = 0$, and we have

$$U_1 = U_{1g} = \frac{B}{\sqrt{\mu\rho}} = U_A \tag{2.26}$$

(2) For transverse propagation $\theta = \frac{\pi}{2}$, we have

$$U_1 = 0 \quad \text{and it is perpendicular to } \underline{k}. \tag{2.27}$$

The second group of waves is obtained from equation (2.23). These waves are neither transverse nor longitudinal. In special cases they become transverse or longitudinal. Such cases will be discussed now. The dispersion relations for these waves are obtained from equation (2.23) as,

$$(U^2 - U_s^2)\left(U^2 - \frac{B_x^2}{\mu\rho}\right) = \frac{U^2 B_y^2}{\mu\rho} \tag{2.28}$$

The quadratic equation has a solution similar to the equation

$$x^2 + px^2 + q = 0$$

$$X = \pm\frac{1}{2}\left\{(-p + 2\sqrt{q})^{1/2} \pm (-p - 2\sqrt{q})^{1/2}\right\}$$

Therefore, we have two more waves

$$U_{2,3} = \frac{1}{2}\left\{\left(U_s^2 + \frac{B^2}{\mu\rho} + \frac{2B_x U_s}{\sqrt{\mu\rho}}\right)^{1/2} \pm \left(U_s^2 + \frac{B^2}{\mu\rho} - \frac{2B_x U_s}{\sqrt{\mu\rho}}\right)^{1/2}\right\} \tag{2.29}$$

Let us write down some more information on these waves, obtained from equations (2.23)

$$v_x = \frac{U B_y b_y}{\mu\rho(U^2 - U_s^2)} \tag{2.30}$$

$$v_y = -\frac{B_x}{\mu\rho U} \cdot b_y \tag{2.31}$$

$$v_z = 0 \tag{2.32}$$

$$b_z = 0 = b_x \tag{2.33}$$

$$p' = U_s^2 \rho' \tag{2.34}$$

$$\rho' = \rho_0 v_x / U \tag{2.35}$$

We see clearly that $\underline{b}$ and $\underline{v}$ are in the plane (x, y), i.e., the plane of (k, B_0), in contrast to wave 1 in which the perturbation $\underline{b}$ and velocity $\underline{v}$ were perpendicular to the

plane of (k, B_o). Also in these waves, oscillations of the density ρ' take part, while in wave 1 it does not. Let us consider the two approximations regarding the strength of the field, along with the special cases of longitudinal and transverse propagation, so that the properties of these two waves may become more clear.

(1) Consider the approximation $\frac{B^2}{\mu\rho} \ll U_s^2$; then equations (2.29) and (2.23) give

(a) For wave 2,

$$U_2 = U_s$$

$$b_y \sim v_x \frac{B_y}{U_s} \simeq \frac{v_x B \sin\theta}{U_s} \qquad (2.36)$$

This shows that in this limit, the second wave becomes an ordinary sound wave with a weak transverse perturbation b_y.

(b) For wave 3,

$$U_3 = U_1 = \frac{B_x}{\sqrt{\mu\rho}} = \frac{B\cos\theta}{\sqrt{\mu\rho}} \qquad (2.37)$$

$$v_y = -\frac{b_y}{\sqrt{\mu\rho}} \; ; \; v_x \simeq 0 \qquad (2.38)$$

Thus wave 3 becomes the Alfven wave, with the difference that $\underline{v}$ and $\underline{b}$ are in the plane of (k, B) and not perpendicular to it. However this approximation is not valid in the magnetosphere. In the magnetosphere the magnetic energy is greater than the kinetic energy. The second approximation is valid in the magnetosphere and will be of interest to our problem.

(2) Now consider another case, where a strong field exists, i.e., $B^2/\mu\rho \gg U_s^2$

We have

(a) For wave 2

$$U_2 = \frac{B}{\sqrt{\mu\rho}} = U_A \tag{2.39}$$

$$v_x \approx \frac{b_y \sin\theta}{\sqrt{\mu\rho}} \; ; \; v_y \approx \frac{-b_y \cos\theta}{\sqrt{\mu\rho}} \tag{2.40}$$

Note that this wave has the same phase velocity as the Alfven wave U_1 when $\theta = 0$. Since it is independent of the direction of $\underline{k}$, the group velocity has the direction of $\underline{k}$. Also

$$U_{2g} = \frac{B}{\sqrt{\mu\rho}} \cdot \frac{\underline{k}}{|\underline{k}|} \tag{2.41}$$

while in the case of wave 1, the group velocity was in the direction of the field $\underline{B}_0$. Also $\underline{v}$ is perpendicular to $\underline{B}$ with the magnitude

$$v = \frac{b_y}{\sqrt{\mu\rho}} \tag{2.42}$$

(b) For wave 3, we have

$$U_3 \sim U_s \cos\theta = U_s \frac{b_x}{|\underline{B}|} \tag{2.43}$$

This wave becomes a sound wave in this approximation propagating at angle θ. The group velocity of the wave is

$$U_{3g} = \frac{\partial\omega}{\partial\underline{k}} = U_s \frac{\underline{B}}{|\underline{B}|} \tag{2.44}$$

and

$$v_x \approx \frac{B}{\rho U_s \mu} \cot\theta\, b_y \tag{2.45}$$

$$v_y \approx \frac{B}{\rho U_s \mu} b_y \tag{2.46}$$

The velocity $\underline{v}$ is antiparallel to $\underline{B}_o$ with the magnitude

$$v = \frac{B^2}{\rho U_s \mu}\left(\frac{b_y}{B_y}\right) \tag{2.47}$$

The above analysis shows that, in the compressible fluid, in addition to Alfven waves where $\underline{v}$ is perpendicular to the plane (k, B), we can have waves in which $\underline{v}$ is parallel to the plane (k, B). Such waves are possible in cases 1 (b) and 2 (a).

However, for the arbitrary relation between B^2 and U_s^2, U_2 and U_3 depend on the angle between $\underline{k}$ and $\underline{B}$[17]. If the angle increases, U_2 increases and U_3 decreases. In general

$$U_3 \leq U_1 \leq U_2; \quad U_2 \geq U_s; \quad U_3 \leq U_s$$

But in special cases,

(a) $\underline{k}$ ll B; B (B, o,o)

$$U_1 = \frac{B}{\sqrt{\mu\rho}} = U_A \tag{2.48}$$

U_2 = greater of U_s and U_1

U_3 = greater of U_s and U_1

(b) $\underline{k} \perp \underline{B}$; B (o, B, o)

$$U_2^2 = U_s^2 + \frac{B^2}{\mu\rho} \; ; \; U_3 = 0 = U_1 \tag{2.49}$$

Thus only one wave exists, which propagates perpendicular to the magnetic field with the combined velocity of sound and Alfven waves. This wave is called magnetoacoustic or magneto-sonic wave. It has a longitudinal disturbance b_y. In approximation 1, it has approximately the speed of sound. In approximation 2, it has the speed of the Alfven wave, but propagates in a direction perpendicular to B_o.

This magneto-sonic wave has great significance in geophysics where perturbations along the field line (longitudinal changes) can be propagated in the direction perpendicular to the magnetic field (transverse propagation).

In contrast, if we have an incompressible fluid, we take $\lim U_s \to \infty$ in equation (2.28) or (2.29), and obtain only one type of wave, the dispersion relation of which is just

$$U_1 = \frac{B_x}{\sqrt{\mu\rho}} \tag{2.20}$$

There is no propagation for $\underline{k}$ perpendicular to $\underline{B}$, but only for $\underline{k}$ parallel to $\underline{B}$. This is the Alfven wave discussed before. The physical explanation of which was given by Alfven, in terms of the tight material string, with $\underline{v}$ and $\underline{b}$ perpendicular to plane of ($\underline{k}$, B). These are two simple cases which give some understanding of hydromagnetic waves. However, in general propagation in arbitrary directions is complicated.

It should be remarked that even when the conditions

$$\omega << \nu_{eff} \; ; \quad \omega_c << \nu_{eff}$$

do not hold, such as in a rarefied plasma ($\nu_{eff} \approx 0$) in the low frequency range $\omega \ll \Omega_i$, the results obtained by the quasi-hydromagnetic approach are the same as discussed above[14].

Let us now consider the detection of these waves by the experimental techniques.

3. Observations of Hydromagnetic Waves

a. Laboratory Experiments. After the theoretical discovery of magnetohydrodynamic waves by Alfven in 1942, the first attempt to observe them in the laboratory was done by Lundquist[8] in 1951. Mercury in a cylindrical stainless steel vessel was subjected to a vertical magnetic field of 13,000 gauss. A horizontal disk with radial strips was fastened to it at the bottom of the mercury. The waves were excited as small torsional vibrations about the vertical axis by moving the disk. The waves travelled upward, were reflected from the upper surface and created standing waves. The experimental results did not agree well quantitativly with theory, therefore the existence of magnetohydrodynamic waves was only qualitativly demonstrated. Mercury has a very high density and because of the finite conductivity ($\rho_m = 13600\,\mathrm{kgm^{-3}}$; $\sigma = 10^6\ \mathrm{ohm^{-1}m^{-1}}$) there were heavy dissipation losses.

Since mercury is not an ideal medium to observe magnetohydrodynamic waves, Lehnert[18] used liquid sodium, ($\sigma = 1.4\times10^7\ \mathrm{ohm^{-1}\ m^{-1}}$). The attenuation was reduced but the results were still not satisfactory.

Bostick and Levine[19] did an experiment using a rarefied ionized gas. The compressibility is important in this case ($U_A >> U_S$) and they observed periodicity in the density. A toroidal tube, with a magnetic field along the tube, prevented diffusion of ions to the walls. Though the waves looked like magnetohydrodynamic waves, other interactions between the electromagnetic field and the material motion were present. The standing waves could not be maintained without an external supply of energy. In this case electromagnetic energy. If the density of the gas is increased, the velocity of the magnetohydrodynamic wave decreases. Also the conductivity of the ionized gas is too low. Recently Wilcox et al did several experiments on these waves in plasma[9]. It is difficult to achieve in the laboratory, as ideal a medium as possible on cosmical scale for hydromagnetic waves, (Section 5, Chapter I).

b. Hydromagnetic Waves on a Geophysical Scale. For a long time, it has been known that the geomagnetic field exhibits small periodic changes. Recently these changes have been studied systematically at many places on the earth. These regular periodic changes with periods ranging from a fraction of a second to several minutes (see Figure 1), on the earth's surface are thought to be a manifestation of hydromagnetic waves originating somewhere in the exosphere. Dungey[2] attempted to consider periods greater than 10 seconds as oscillations of matter of exosphere in the earth's magnetic field. Several other workers have done detailed

theoretical work following Dungey. This will be the subject of a detailed discussion in Chapter IV.

To observe such waves, the effect of nuclear explosions at high altitude was studied by Bomke et al[20] and Maeda and Ondoh[21]. Bomke identified the modified Alfven and transverse waves produced by the high altitude Argus experiment. Maeda and Ondoh observed a similar effect from the Johnston Island nuclear explosion. Very convincing evidence of a train of hydromagnetic waves was obtained by Sugiura[3] from ground magnetometer records. He found that waves of 4 to 8 minutes existed at conjugate points of the earth: College, Alaska and Macquarie Island. He identified the damped waves at northern and southern points as hydromagnetic waves generated at 5 or 6 earth radii and propagated in a longitudinal mode of propagation along the field line. He also showed that these transverse waves are elliptically polarized. His very detailed study of these waves was also applied to the sudden-commencement theory of magnetic storms[22].

Recently Nagata et al[23] confirmed the work of Sugiura by using another pair of conjugate stations in the southern and northern hemispheres and showed that micropulsations of 6 minute periods existed in both hemispheres simultaneously. Following the availability of earth satellites, magnetic field measurements in outer space were possible. The first such study of hydromagnetic waves was done by Sonett et al with Pioneer I[24]. They identified magnetoacoustic, oblique and transverse waves at the geocentric

distance of 3.7 to 7.0 earth radii on the sunward side of the magnetosphere. Several frequencies extending up to $\omega = 13$ rad/sec were found. This was the first direct evidence of such waves in the magnetosphere. Similar results were obtained by Coleman et al with Pioneer V[25]. However, the results were somewhat qualitative.

Later, Judge and Coleman[26] observed low frequency hydromagnetic waves of 100 to 500 second period with Explorer VI ($f = 10^{-2}$ to 0.2×10^{-2} cps, $\omega = 6.28 \times 10^{-2}$ to 1.256×10^{-2}). They found that the transverse mode had a period of 200 seconds, and was elliptically polarized, while the compressional wave had a period of 100 seconds.

Though evidence of the existence of hydromagnetic waves was established by these measurements, only the component of the magnetic field perpendicular to the spin axis of the satellite was measured. The aspect indicator allowed determination of the direction of this component with respect to the sun. Only two out of three parameters needed to know the ambient field were available. Therefore the information available was not sufficiently complete to determine the ambient field. The effect of these waves on the earth's field at the ground level was not investigated. Our intent is to study hydromagnetic waves using direction and magnitude of the ambient magnetic field available from the Explorer XII satellite magnetometer experiment. The results will then be compared with the information obtained from ground magnetometer records. In the next chapter, some details on the orbit of the satellite, principles of the

magnetometer, and a detailed procedure of studying these waves are described.

CHAPTER III

DETECTION OF HYDROMAGNETIC WAVES IN THE MAGNETOSPHERE BY EXPLORER XII SATELLITE

1. Coordinate System and the Method of Measurements of the Magnetic Field in Space

The Explorer XII satellite was equipped to measure the total vector magnetic field inside the magnetosphere and in the vicinity of the termination of the geomagnetic field. Figure 2 gives the position of its orbit in the magnetosphere. The orbit was elliptical with eccentricity ϵ=0.854 and was inclined to the equator of the earth by 33°. The perigee was approximately 7600 km and apogee , 83,000 km (> 13 R_e). The major axis made an angle of a few degrees with the noon meridian when the satellite was launched on August 16, 1961 at 0330 U.T. A schematic diagram is shown in Figure 4. Since the orbit was fixed in the space but was carried with the earth around the sun, the angle between the major axis and the noon meridian increased as time progressed (approximately 1° per day). The magnetosphere is supposed to be symmetrical about the sun-earth line or slightly rotated from this line depending upon the direction of the "solar wind". Thus during the four month lifetime of Explorer XII a considerable portion of the magnetosphere was examined. The spin axis of the satellite was fixed in space with celestial coordinates:

Right Ascension $= 47^{o}$

Declination $= -27.5^{o}$ (1.1)

The magnetometer used on the satellite was a flux-gate type. The principle of operation of this magnetometer[27] is reviewed in Appendix D. Other types of magnetometers are also used in space research; their principles and limitations are discussed in a review paper by Cahill[28].

The flux-gate magnetometer used in this experiment had three elements arranged along mutually perpendicular axes. This arrangement allowed measurement of three components of the magnetic field. One element was parallel to the spin axis and was labelled as the Z-axis. The other two elements mutually perpendicular, formed X and Y axes in the plane perpendicular to the Z axis. The (X,Y) plane rotated with the satellite spin rate ($\sim$30 RPM). A vector magnetic field measurement was available three times every second. Since the orthogonal sensor system rotates around Z axis, it is not a very convenient frame for interpretation of results. We define the vector field with respect to two reference axes which are fixed in space. One such axis is the Z axis itself and we can find the angle it makes with vector field $\underline{B}$. Another, slowly changing, reference axis is the line joining the sun and the satellite. The angles are defined with respect to these two axes. The angle α is between the Z axis and $\underline{B}$, and ψ is the angle between two planes: One formed by the Z axis and $\underline{B}$ and another formed by the Z axis and the sun line. The magnetic field vector is completely defined by the angles α,

and ψ and the magnitude B. The angles are like zenith and azimuth in a satellite system of coordinates (see Figure 4). Finally, B, α, ψ are calculated by an electronic computer with the help of programs developed by the author using the formulas:

$$B = (B_x^2 + B_y^2 + B_z)^{1/2} \tag{1.2}$$

$$\alpha = \cos^{-1}\left(\frac{B_z}{B}\right) \tag{1.3}$$

$$\psi = 307^\circ + \omega\Delta t + \tan^{-1}\left(\frac{B_y}{B_x}\right) \tag{1.4}$$

where ω is the spin rate and Δt is time interval between two successive readings (o.333 sec.). The complete details of data reduction and its limitations are given in a paper by Cahill and Amazeen[29] and will not be repeated here.

The above satellite-oriented coordinate system is very convenient to reduce information from the satellite data, but is not suitable to study the variation of the geomagnetic field and subsequently, hydromagnetic waves in the magnetosphere. We should have the magnetic field measurement in a geocentric coordinate system. A procedure has been developed by the author, using the celestial sphere to transform vector magnetic field measurements from the satellite B, α, ψ coordinate system to the geocentric coordinate system. This is given in detail in Appendix E. In geocentric spherical coordinate system three components B_r, B_θ, and B_ϕ are obtained where B_r is along the radius vector toward the center, B_θ is upward and B_ϕ along increasing east longitude. These three components are used

to study the hydromagnetic waves in different modes of propagation.

2. Method of Detection of Hydromagnetic Waves

As discussed in Chapter II, one effect of the hydromagnetic waves will be a variation in the ambient magnetic field in the ionized gas. In the present problem the ambient magnetic field is the magnetic field of the earth, and the ionized gas present in the magnetosphere is the medium. The magnitude of this field in the region of the magnetosphere where we shall be working is 150 to 200 γ ($\gamma = 10^{-5}$ gauss). The variations in this field which we shall study will be of the order of 10 γ. (This allows linear treatment of the theory, since $b \ll B_0$). However, to detect such a small change a very careful procedure is necessary. The following method is used to bring out clearly the effects of the hydromagnetic waves.

We have seen in Section I that information about the geomagnetic field is obtained in terms of B, α, ψ. The errors in these quantities should be considered. The main part of the error comes from the digitization of the original data. This is $\pm$ 12 gamma in each component X, Y and Z. From the preceeding discussion it is known that X and Y rotate with the rate of satellite spin and therefore the X and Y components of steady transverse field component will be scattered through the different digitization "windows" in a somewhat random fashion. The Z axis component is different for a steady field component along this axis,

the measurement remains in one window while the Z component changes by 23 gammas. If we select data where Z axis has a very small component then the errors in Z are less significant and we can treat the errors in X and Y as random. The errors are still considerable, though approximately random, therefore the data is averaged over 15 seconds interval (nearly 50 points). This removes much of the scatter due to digitization and typical errors in the averages of B, α and ψ computed in a sample of data are as $\pm$ 3 γ, and 5 to 6 degrees respectively.

After obtainly B, α, ψ for every 15 seconds, these values are used to compute B_r, B_θ , B_ϕ , by the method described in Appendix E. All these computations are carried out on IBM 1620 computer. In order to further reduce data scatter we have smoothed B_r , B_θ , and B_ϕ by taking sliding, or running averages over a period of one minute. Finally, we have three orthogonal components B_r, B_θ , and B_ϕ each of them having uncertainties of approximately 3 to 4 γ. These components are used to separate the modes of propagation of the waves.

3. Separation of Transverse and Longitudinal Modes of Propagation of Hydromagnetic Waves

a. Waves in Anisotropic Conducting Medium. Theoretical treatment of hydromagnetic waves in compressible medium is very complicated to study. A further complication is added when we consider an anisotropic medium. In the previous treatment we assumed that the conductivity of the gas is a constant, i.e., the same in all directions. As

calculated in Appendix B, this is not the actual case. We should consider the conductivity as a tensor. The problem now becomes very difficult to solve when we consider propagation of waves at any arbitrary angle. However, we can introduce certain special conditions which are valid in our case to reduce the complication. We assume that the magnetic pressure is much greater than the gas pressure, i.e.,

$$\frac{B^2}{\mu} >> U_s^2 \tag{3.1}$$

This is indeed the case in the magnetosphere where the Alfven velocity is 500 km/sec compared to a sound velocity 20 km/sec. Piddington[30] has shown that the dispersion equation becomes simple with this assumption. He has further shown that in anisotropic media the waves are circularly polarized when they propagate along the direction of the field and become elliptically polarized when the direction of propagation is inclined. They become plane polarized when the angle θ is $\pi/2$. This feature was hidden in the treatment of isotropic medium. Since the medium in the magnetosphere is anisotropic, we should modify the theoretical treatment in Chapter II. (See Appendix B where it is shown that the Hall conductivity σ_2 is much greater than Pedersen conductivity σ_1). Therefore, before we separate the different modes of propagation of hydromagnetic waves this modification should be made. In doing so we shall be able to derive the polarization of the waves.

The first step is to rewrite Ohm's law as

$$\underline{J} = \sigma_0 E_{\parallel} + \sigma_1 E_{\perp} + \sigma_2 \frac{\underline{B} \times \underline{E}_{\perp}}{B} \tag{3.2}$$

where σ_0 is the direct conductivity, σ_1 is the conductivity perpendicular to $\underline{B}$ (Pedersen conductivity) and σ_2 is the Hall conductivity in the direction perpendicular to $E_{\perp}$ and $\underline{B}$. Following Piddington[30] and the notations for the coordinate system of Chapter II, but where the unifrom magnetic field, B_0, is taken along X axis, we combine

$$\underline{J} = \sigma(\underline{E} + \underline{v} \times \underline{B}) = \sigma \underline{F}$$

with Maxwell's equation, neglecting displacement current,

$$\nabla \times \underline{H} = \underline{J}$$

Considering these component by component with algebraic manipulation and assuming

$$\underline{B} = \underline{B}_0 + \underline{b}$$

where $b \ll B_0$, we have

$$\frac{\partial^2 b_x}{\partial y^2} + \frac{\partial^2 b_x}{\partial x^2} = \sigma_3 \mu \left(\frac{\partial b_x}{\partial t} + B_0 \frac{\partial v_x}{\partial y} \right) + \frac{\sigma_2}{\sigma_1} \frac{\partial^2 b_z}{\partial x \partial y} \tag{3.3}$$

$$\frac{\sigma_3}{\sigma_0} \frac{\partial^2 b_z}{\partial y^2} + \frac{\partial^2 b_z}{\partial x^2} = \sigma_3 \mu \left(\frac{\partial b_z}{\partial t} - B_0 \frac{\partial v_z}{\partial x} \right) + \frac{\sigma_2}{\sigma_1} \left(\frac{\partial^2 b_y}{\partial x^2} - \frac{\partial^2 b_x}{\partial x \partial y} \right) \tag{3.4}$$

$$\frac{\partial^2 b_y}{\partial y^2} + \frac{\partial^2 b_y}{\partial x^2} = \sigma_3 \mu \left(\frac{\partial b_y}{\partial t} - B_0 \frac{\partial v_y}{\partial x} \right) - \frac{\sigma_2}{\sigma_1} \frac{\partial^2 b_z}{\partial x^2} \tag{3.5}$$

$$\sigma_3 = \sigma_1 + \frac{\sigma_2^2}{\sigma_1} \tag{3.6}$$

Note that the term containing $\frac{\sigma_2}{\sigma_1}$ is responsible for elliptical polarization. Since $\frac{\sigma_2}{\sigma_1} \sim 10^7$, the medium in the magnetosphere is anisotropic (see Appendix B).

Now consider the wave propagated along the axis

making an angle θ with X axis in XY plane and assume the solutions

$$e^{i(\underset{\sim}{k}\cdot\underset{\sim}{r}-\omega t)} \tag{3.7}$$

We should substitute in the foregoing equations, together with hydrodynamic equations, the following

$$\begin{aligned}\frac{\partial}{\partial x} &= ik\cos\theta \\ \frac{\partial}{\partial y} &= ik\sin\theta \\ \frac{\partial}{\partial t} &= -i\omega\end{aligned} \tag{3.8}$$

without going into cumbersome general treatment, we simplify with assumstion (3.1), and eliminating v_x , v_y , v_z , we get the modified equations.

$$(k^2+i\epsilon_0\omega^2-i\epsilon_0 U_A^2k^2)b_y+\frac{\sigma_2}{\sigma_1}\cos^2\theta\, k^2 b_z=0 \tag{3.9}$$

$$(k^2+i\epsilon_0\omega^2-i\epsilon_0 U_A^2\cos^2\theta)b_z-\frac{\sigma_2}{\sigma_1}k^2 b_y=0 \tag{3.10}$$

also,

$$(\omega^2-U_s^2\sin^2\theta k^2)v_y-U_s^2\sin\theta\cos\theta k^2 v_x+\frac{U_A^2 k\omega}{B_0\cos\theta}b_x=0 \tag{3.11}$$

$$\omega v_z+U_A^2\frac{\cos\theta k}{B_0}b_z=0 \tag{3.12}$$

$$(\omega^2-U_s^2\cos^2\theta k^2)v_x-U_s^2\sin\theta\cos\theta k^2 v_y=0 \tag{3.13}$$

where,

$$\epsilon_0=\frac{\mu\sigma_0}{\omega}\quad ;\quad U_A^2=\frac{B_0^2}{\mu\rho_{in}}$$

We have assumed that only electron conductivity is important, i.e. $\sigma_0=\sigma_3$. In order to study polarization of hydromagnetic waves we use

$$\frac{b_z}{b_y}=\frac{R}{\cos\theta} \tag{3.14}$$

Eliminating b_y and b_z from equations (3.9) and (3.10) we have

$$R^2 - i\epsilon \frac{\sigma_1 U_A^2 \sin^2\theta}{\sigma_2 \cos\theta} R + 1 = 0 \qquad (3.15)$$

Therefore,

$$R = \frac{i}{2}\left\{\frac{\Omega_i \sin^2\epsilon}{\omega \cos\theta} \pm \left(\frac{\Omega_i^2 \sin^4\theta}{\omega^2 \cos^2\theta} + 4\right)^{1/2}\right\} \qquad (3.16)$$

We have two elliptically polarized waves. When $\theta = \frac{\pi}{2}$, the waves are plane polarized. In intermediate directions, the waves are elliptically polarized.

The value of R that determines the polarization of the waves is dependent on $\frac{\Omega_i}{\omega}$ and angle θ . Hydromagnetic waves of period of 100 sec in the magnetosphere have value $\frac{\Omega_i}{\omega} = 10^3$ (see Appendix B). For a very large value of $\frac{\Omega_i}{\omega}$ the waves will be plane waves. In our case, the waves are circularly polarized for $\theta = 0$. The waves become highly elliptical (R = 10) when $\theta \approx 10^\circ$. As the angle θ increases more than 10°, the waves are linearly polarized. We shall separate these three kinds of polarizations in the magnetosphere.

b. Separation of the Modes. It is obvious from the previous treatment that identification of the hydromagnetic waves in the geomagnetic field is still not possible. The main problem is that we do not know the angle θ ; also the experimental observations are not controllable, i.e., there may be several waves propagating along

different directions. For this reason we make the further simplifications that we shall look for waves, (1) propagating along the line of force, i.e., $\theta = 0$ or somewhat close to it, and (2) propagating across the field lines, i.e., $\theta = \frac{\pi}{2}$.

The first wave would be circularly polarized, or elliptically polarized if θ is non-zero, and perturbation in $\underline{B}_o$ would lie in a plane perpendicular to the direction of $\underline{B}_o$. If we know two components of the perturbation $\underline{b}$ in this plane, the combination of b_y and b_z, for example, should give us information on the polarization of these transverse waves.

In order to study these transverse waves in the magnetosphere, we use the components B_r, B_θ, and B_ϕ already discussed in Section 2 of this Chapter. We have selected data near the geomagnetic equator. The main field is along B_θ and B_r and B_ϕ now lie in the plane perpendicular to B_θ which may be taken as $\underline{B}_o$. The problem now is very much simplified. Therefore, transverse hydromagnetic waves are obtained by combining fluctuations in B_r and B_ϕ near the geomagnetic equator from Explorer XII data. Vector diagrams formed by this method give the amplitude, period, and sense of polarization of the transverse waves.

The second kind of waves, which may be called longitudinal or magnetosonic waves, are propagating across the field lines. These waves are plane polarized. The perturbation in the ambient field, near the equator, is in

B_θ . Study of variations in B_θ should provide information on these waves. The general procedure described in Sections 2 and 3 is followed to study these modes of propagation of hydromagnetic waves in the magnetosphere. The results of this study are discussed in the next chapter.

CHAPTER IV

AMPLITUDES, FREQUENCIES AND POLARIZATION OF THE HYDROMAGNETIC WAVES IN THE MAGNETOSPHERE

1. Alfven Waves

We have discussed in Chapter II three types of waves possible in a conducting compressible medium in the magnetic field. We shall consider two special cases of these waves. One kind of the wave propagates along the field line and another kind of the wave propagates across the field line. The detailed procedure described in Chapter III readily enables us to separate these two modes from the Explorer XII data. In this section we shall discuss the results of the Alfven waves propagating along the field line. We know from the previous discussion that the medium with which we deal has $\sigma_z \gg \sigma_r$, and therefore is anisotropic. This would mean that the waves will be circularly polarized when the wave vector $\underline{k}$ is along $\underline{B}_o$, and elliptically polarized if $\underline{k}$ makes a small angle with $\underline{B}_o$. In this study, we will discuss typical frequencies, amplitudes and polarizations.

We follow the method described in Sections 2 and 3 of Chapter III. By this method, we have three perpendicular components B_r, B_θ, and B_ϕ of the ambient field. In order to define the direction of the rotation of the perturbation vector $\underline{b}$, we should define the directions of three components. B_r is toward the center of the earth,

B_θ pointing north and B_ϕ eastward.

Since we have no precise knowledge of the unperturbed field, there is no direct way to find perturbation b. We shall, therefore, plot the field components perpendicular to the main field and study the relative changes. In this study observations were considered close to the geomagnetic equator (less than 10°), therefore the main field is very closely along B_θ and the transverse perturbation is in B_r and B_ϕ . A typical example is given in Figure 7. Combining B_r and B_ϕ we should get the vector perturbation b for these waves. The rotation of this vector b gives the polarization of the wave. Several examples of such waves are discovered in the magnetosphere at various radial distances and longitudinal positions.

a. Amplitudes and Frequencies. Several examples of transverse Alfven waves were obtained in the magnetosphere ranging from 43,000 km to 67,000 km in radial distance. They were observed at various latitudes and longitudes. An attempt was made to cover the magnetospheric region from sun-earth line to approximately 75° on the dawn side (1200 to 0700 local time), Most of the observations included in this study were close to the geomagnetic equator. Eight examples of these waves are shown in Figure 8. Complete information about the amplitudes, frequencies (periods), the location (local time, latitude, etc.) where these waves were observed are summarized in Table 1 (p. 50). We wish to examine all these examples of transverse waves in detail and to see if some consistent pattern of their properties

can be found.

In Figure 8 (1)(September 14, 1961) the wave is nearly circularly polarized with an amplitude of 8 gammas. From Chapter III, Section 3, it follows that this wave propagates just along the field line and the disturbance vector $\underline{b}$ is equally divided into the two components along B_r and B_ϕ .

In Figure 8 (2) (September 14, 1961) the wave is elliptically polarized. This indicates that the wave vector $\underline{k}$ makes a small angle with the direction of $\underline{B}$. (The component perturbation along B_r is greater (7 gammas) than that along B_ϕ (3 gammas).) The application of equation (3.16) of Chapter III indicates that the wave propagates at an angle less than 10°. Both of these examples are near 1200 hours local time.

The waves shown in Figures 8 (3) and 8 (4) were observed on September 30, 1961 at approximately 1100 hours local time. In both of these cases the largest perturbation is along B_r (10 gammas) and much smaller along B_ϕ (4 gammas). Figure 8 (4) shows the largest amplitude observed (11 gammas). The elliptical polarization indicates that the wave propagates at an angle of about 10° with the magnetic field lines. The third example at this local time is shown in Figure 8 (5) on October 8, 1961. This elliptically polarized wave has amplitude of 7 gamma along B_r, larger than that along B_ϕ .

One general observation that emerges from these examples is that the largest part of the perturbation in the

TABLE 1

TRANSVERSE HYDROMAGNETIC WAVES : EXPLORER XII

	DATE 1961	AMPL. (GAMMAS)	PERIOD (SEC)	LOCAL TIME	DISTANCE x 10^3 KM	LATITUDE GM	POLARIZATION	BOUNDARY LOCATION x 10^3 KM
1.	September 14	8	135	1200	50.0	+8.0	Anticlockwise	56.0
2.	September 14	8	150	1200	50.0	+8.0	Anticlockwise	56.0
3.	September 30	4	150	1100	51.0	+3.0	Anticlockwise	67.5
4.	September 30	11	180	1045	54.5	+1.0	Anticlockwise	67.5
5.	October 8	7	120	1045	43.0	-2.5	Clockwise	65.0
6.	October 25	10	100	0920	52.0	+8.3	Clockwise	
7.	October 25	9	100	0906	54.4	+7.6	Clockwise	
8.	November 25	6	120	0650	67.6	+6.0	Clockwise	

TABLE 2

LONGITUDINAL HYDROMAGNETIC WAVES: EXPLORER XII

	DATE 1961	AMPL. (GAMMA)	PERIOD (SEC)	LOCAL TIME	DISTANCE x 10^3 KM	LATITUDE GM	POLARIZATION	BOUNDARY LOCATION x 10^3 KM
1.	September 21	7	200	0800	53.0	-30.0	Linear	67.0
2.	October 1	8	150	1028	64.0	+1.0	Linear	
3.	August 27	4	150	1300	48.0	+2.2	Linear	

magnetic field is along B_r, at 1100 - 1200 local time.

Figures 8 (6) and 8 (7) represent waves observed on November 25, 1961 at 0900 hours local time. The major part of the perturbation field $\underline{b}$ is along B_ϕ (10 gammas). Figure 8 (8) also represents the similar observation at local time 0700 hours. Near the sun-earth line, the amplitude has the larger component along B_r while waves produced at large angles from the sun-earth line have the larger component along B_ϕ.

This important observational fact regarding dependence of the amplitude on local time suggests that the mechanism for the generation of the hydromagnetic waves in the magnetosphere is related to the "solar wind" flowing around the magnetosphere. Near the sun-earth line, the changes in the solar wind pressure affect the B_r component of the magnetic field. At an angle of 75° from the sun-earth line, the solar wind flows tangentially to the magnetospheric surface and some force (perhaps viscous) is apparently exerted along the B_ϕ direction. Quantitative work utilizing this observation in the mechanism of generation of these waves will be discussed in Chapter V.

The period of the waves found from these eight examples is of the order of 100 to 200 seconds. However, it should be mentioned that the errors involved in the data require averaging and smoothing of the data over a period of 60 seconds. We cannot obtain waves of smaller period than 60 seconds. The examples studied suggest that a 100-200 second period is predominant. Previous work of Judge

and Coleman[26] and Sonett[31] also find the similar values of the periods of the hydromagnetic waves in the magnetosphere. Therefore the waves of 100-200 second period seem to be usual phenomena in the magnetosphere.

Previous work on the hydromagnetic waves was based on the incomplete information of the ambient magnetic field (see p.). Because of this reason it was not possible to find the total amplitude and all of the components. The important feature in the present study about the dependence of the magnitude of the two components along B_r and B_ϕ on local time was not revealed. This fact certainly will help us to understand the mechanism of the generation of these waves and the interaction of the solar wind at the magnetospheric boundary. Now, we shall study the direction of the rotation of the perturbation vector in these waves.

b. Polarization: Local Time Dependence. The polarization of the hydromagnetic waves can be obtained in each of eight cases discussed above (See Figure 8). The directions of the rotation of the perturbation vector are taken directly from Figure 8 and tabulated in Table 1 (p. 50). The sense of the rotation assigned is of an observer looking down from above the north pole. This system is used because we shall discuss the mechanism of the generation of these waves at magnetosphere solar wind boundary. A view looking down on the magnetosphere is appropriate to the discussion.

An interesting observation about the polarization of the waves is their dependence on the local time, i.e.,

the longitudinal distance from the sun-earth line. From Table 1, we conclude that during the local time interval of 0700 to 1100 hours the polarization is clockwise and after 1100 hours it is anticlockwise. Since the satellite was launched in an orbit with the major axis initially along sun-earth line and major axis rotated toward morning side, measurements on the evening side are not available.

The dividing line between clockwise and anticlockwise polarization is not the sun-earth line, 1200 hours, but is apparently 1100 hours. This is also the case for several geophysical phenomena observed on the ground. Wilson and Sugiura[22], while studying sudden commencement (SC) geomagnetic storms, found that if SC were interpreted as a transverse wave propagating along the lines of force and arriving in high latitudes, the polarization of SC showed a strong local time dependence. They found that looking down from the north pole, the polarization, at ground level, is clockwise from 1000 - 2200 hours and anticlockwise from 2200 - 1000 in the northern hemisphere. The dividing line was approximately 1000 hours. Nagata et al[23] studying giant pulsations on the ground, found the dividing line near 1100 hours. Several other phenomena, such as polar S_q and D_s current systems indicate the same tendency. The results of this study are the first indication of similar behavior at satellite ($5\text{-}10R_E$) altitudes.

The waves we have found are not giant pulsations (decaying large amplitude waves) or SC perturbations, but rather small pulsations. All three phenomena of these are

actually transverse hydromagnetic waves, and they should show similar characteristics.

The opposite direction of the polarization of transverse waves about the symmetry line suggests that the flow of the solar wind around the magnetospheric surface is the cause of such waves. A qualitative view can be seen in Figure 9. According to this view looking down from the north pole, a wave of clockwise polarization in space traveling along a line of force would arrive at the earth's surface in the high north latitude and would appear anticlockwise. Since the direction of the line of force is reversed, in passing from the equator to the surface, an anticlockwise wave in space will become clockwise on the earth. Before we work out a quantitative theory for the generation of these waves, we should check this prediction by comparing simultaneous observations in space and at ground level. Since this has never been done, we have tried to do this for Explorer XII data.

c. Effects on the Geomagnetic Field at the Earth's Surface. Hydromagnetic waves which were assumed to be generated in the magnetosphere and propagated along the lines of magnetic field were observed on the surface of the earth by Sugiura[3] and Nagata et al[23] using ground magnetogram records. Judge and Coleman[26] interpreted their data from Explorer 6 as transverse elliptical waves, but did not show corresponding ground records. Both of these observations provide inconclusive evidence of hydromagnetic waves propagating from the magnetosphere to the ground unless we

have evidence of the same wave in the magnetosphere and on the ground. In order to detect hydromagnetic waves which are generated in the magnetosphere and propagated along a line of force to the observatory on the surface of the earth, the satellite and the observation must be on the same line of force. The satellite should be close to the longitude of a ground station where continuous record of the earth's field is available. This requirement has made correlation difficult. We have found that when there is a significant wave in the ground records and satellite observations were made 60° away longitudinally, waves in the satellite record were not found. The waves found were small, i.e., 10 gamma amplitude, and it may be that they are quite local in longitudinal extent, 10 to 20 degrees. When there are waves on the ground records, we should have the satellite measurements available at a location within 10° to 20° longitude of the ground station and approximately on the same field line (same L value).

We have been able to find two examples of hydromagnetic waves when the satellite was very close to the longitude of College, Alaska (within 10°) on September 14, 1961. Waves of amplitude 8 gamma were found in the satellite record. The simultaneous record of the magnetic field at College, Alaska was examined. Combining the values of ΔH and $H\Delta D$ from the College rapid run magnetogram we found the effects of these waves very clearly. The results are shown in Figure 10.

Comparison of satellite and ground observations

indicates that looking down from the north pole, the anti-clockwise wave at 1200 hours local time in space is manifested as clockwise wave on the ground[33]. Further support is obtained by the fact that there is a one and one half minute delay between the satellite observation and the ground observation presumably due to travel time along the line of force shown by the satellite vector diagrams. The pattern of disturbance is quite well reproduced in the ground record. The amplitude is slightly decreased but due to errors in the measurements (order of $\pm$ 3γ) we cannot comment on this with confidence.

We have these two examples as the first direct evidence of the fact that hydromagnetic waves do originate in the earth's magnetosphere and propagate along the lines of force to the earth's surface. With this support from the observations, we shall develop a model for the generation mechanism of these transverse waves.

2. Magnetosonic Waves

In Chapter II, it is shown that the modified hydromagnetic wave (it becomes an ordinary hydromagnetic wave, Alfven wave, when $\theta = 0$ or $\underline{k} \parallel B$, equations 2.46 and 2.48) and the modified sound wave, or magnetosonic wave, do not generally propagate precisely longitudinally or transversely. Since it is difficult to interpret the effects of these waves traveling at arbitrary angles some simplifications are necessary. In the case of hydromagnetic waves, therefore, only waves propagating longitudinally were investigated and

several cases were found. If we assume that $\underline{k}$ is perpendicular to $\underline{B}$ in the case of modified sound waves, it becomes much easier to identify them. From Chapter II, we have a magnetosonic wave propagating across the field line with velocity (Equation 2.49).

$$U_2^2 = U_S^2 + \frac{B^2}{\mu\rho} = U_S^2 + U_A^2 \qquad (2.1)$$

Since in the magnetosphere $U_S \ll U_A$ we have,

$$U_2 = \frac{B}{\sqrt{\mu\rho}} = U_A \qquad (2.2)$$

The perturbation created by this wave motion is along the field lines. The velocity of the wave is approximately that of ordinary Alfven wave but the wave has entirely different characteristics. It propagates across rather than along the field lines and thus causes rarefaction and compression of the field lines. We should see the periodic changes principally in the magnitude of the field.

In past, these waves have been investigated using Pioneer I and Explorer VI observations in the magnetosphere. Sonett et al[24] found waves of smaller period (0.5 sec) and Judge and Coleman[26] found waves of the order of 100 seconds. Since these observations were discussed for only one pass and from incomplete information available for the magnetic field, we have tried to study these waves at various locations in the magnetosphere.

The method followed is the same as described in Chapter III, Section 2. After averaging B, α, ψ over 15

second periods, a transformation was carried out as given in Appendix E to obtain B_r, B_θ , B_ϕ . These components are smoothed over one minute period. Since we are close to the geomagnetic equator when these waves are studied, the unperturbed field is along B_θ . We need to study the variation in B_θ only.

The waves are studied from 48,000 km to 64,000 km geocentric distance and at various local times on the dawn side of the magnetosphere. Three very clear examples are shown in Figure 11 and information regarding their amplitude, period, and location is given in Table 2 (p. 51). The waves (2) and (3) in Figure 11 are observed very close to the geomagnetic equator, therefore the perturbations in B_θ are all due to magnetosonic waves.

In Figure 11 (2) on October 1, 1961, the amplitude is quite large (8 gammas), this is the time of the main phase of the geomagnetic storm which started on September 30, 1961 at 2109 UT. The magnetosphere was subjected to heavy perturbations during this time that can be seen by the satellite observations plotted for the whole orbit[34]. It is very likely that these compressional waves were produced by large changes in the solar wind pressure during the storm. This is one effect which might be expected due to solar wind on highly (magnetically) disturbed days. On August 27, 1961, which is less distrubed than October 1, 1961, the waves are of smaller amplitudes (4 gammas). This may be considered as the normal perturbation in the magnetosphere due to solar wind fluctuations.

The wave observed in Figure 11 (1) is at - 30 geomagnetic latitude and so unperturbed field is not entirely along B_θ but the compressional waves should still be observable in B_θ . The large amplitude observed there may not be entirely due to compressional wave. This day (September 21, 1961) is also a magnetically disturbed day, but not as disturbed as October 1, 1961. Though these three examples cannot tell us about oscillations of the entire magnetosphere, we certainly have some general picture of the periodic changes of the magnetic field in the magnetosphere.

In the magnetosphere of the earth, compressional magnetosonic waves of order of 10 gamma amplitude and 150 to 200 second period have been found. Judge and Coleman[26] also found waves of this type with period of 100 sec. Our data processing system does not allow detection of waves with smaller periods than this. These compressional waves can be understood, at least qualitatively as compressional perturbations imparted by fluctuations in solar wind pressure at the magnetospheric boundary.

CHAPTER V

A MODEL FOR THE GENERATION OF HYDROMAGNETIC WAVES IN THE MAGNETOSPHERE

1. Introduction

The study of hydromagnetic waves in the exosphere of the earth was initiated by Dungey[2] who considered the oscillations of the exospheric matter in the earth's magnetic field. The normal modes of oscillation were computed assuming an axially symmetrical model. Several refinements in this model were done by Kato and Akasofu[35] and later on by Watanabe[36]. This model explains some features of the micropulsations observed on the surface of the earth. However, the identification of the several modes of the oscillations with surface observations is difficult. The transverse hydromagnetic waves obtained in Chapter IV do not seem to be micropulsations, but short-lived, small, local perturbations. Therefore, Dungey's model of oscillations of the entire magnetosphere cannot explain the hydromagnetic waves studied in Chapter IV.

Another possibility for the generation of hydromagnetic waves is the direct interaction of the solar wind and the magnetosphere surface. Surface hydromagnetic waves may be generated in the same way as the waves generated at the surface of discontinuity of motion of two fluids in hydrodynamics[37]. The transverse hydromagnetic waves generated

in this manner will travel along lines of magnetic field close to the boundary of geomagnetic field ($\sim$10 R_E). They will arrive in the earth's surface at very high latitudes. These waves cannot travel across the field lines. A third mechanism to consider is the highly irregular conditions[28] (presumably due to fluctuations in solar wind pressure) in the vicinity of the boundary of the magnetosphere as an ensemble of transverse and magnetosonic waves. It is shown by Fejer[38] that a modified Alfven wave or a magnetosonic wave can generate pure transverse and compressional waves by refraction at the boundary. In this way the transverse hydromagnetic waves can be generated at the edge of the magnetosphere. Again they will follow the lines of force near the edge and will arrive at the earth's surface.

All these possible mechanisms do not explain how the transverse hydromagnetic waves can be generated as deep as 7 R_E in the magnetosphere. It is probably true that waves generated by the last two mechanisms can produce waves arriving at earth's surface at 70 to 80 degrees latitude.

In order to explain the hydromagnetic waves observed inside the magnetosphere a new model will be given. This model should explain the following main features of these transverse hydromagnetic waves:

(a) Generation of the waves inside the magnetosphere (7 to 10 R_E)

(b) Opposite polarizations about the symmetry line of afternoon and morning zones.

(c) Rotation of symmetry line toward morning side by 22 degrees (approximately 1100 hours local time).

The last two main features were also observed by Wilson and Sugiura[22] in the study of SC geomagnetic storms and by Nagata et al[23] in the study of giant micropulsation in the ground magnetometer records. Following the suggestion of E. N. Parker, Wilson[39] attempted to explain generation of the hydromagnetic wave associated with the SC by the arrival of a shock wave. The passage of a shock wave near the earth generated hydromagnetic waves of opposite polarizations. The rotation of symmetry line was explained as the inclined direction of arrival of the shock. However, the hydromagnetic waves observed in Chapter IV are not associated with the SC storms and thus are somewhat different phenomena. Another associated geophysical phenomena exhibiting these characteristics is D_s current system in the ionosphere. Any model suggested for transverse waves should be unified with these similar phenomena. Axford[40] has suggested that certain features of the interactions of the solar wind with the magnetosphere are permanent and they are simply enchanced when the geomagnetic storm occurs by the arrival of more plasma. In order to explain the main features of associated phenomena, the model suggested for the generation of the hydromagnetic waves in quiet geomagnetic conditions makes use of this suggestion. We shall assume that in non-storm conditions (quiet geomagnetic conditions) continuous flow of the plasma around the mag-

netosphere creates a "viscous interaction". Due to this viscous interaction magnetospheric motions are introduced inside the magnetosphere. We shall discuss the main features of these magnetospheric motions and viscous interaction in the next section. Since our model for the hydromagnetic waves is based on these ideas, it is very important to understand them.

2. Viscous Interaction and the Magnetospheric Motions

Axford and Hines[41] have advanced a theory of "viscous" interaction of the solar wind and the magnetospheric boundary. They have suggested that by this interaction circulatory motions can be set up inside the magnetosphere similar to those in a falling rain drop. This theory can explain several features of the geomagnetic storms, aurora and D_s current systems. These geophysical phenomena strongly suggest that such circulatory motions may exist in the magnetosphere. During high geomagnetic phenomena these conditions in the magnetosphere are enhanced. In normal quiet geomagnetic conditions, the magnetosphere in the equatorial view looks as shown in Figure 12.

The observations support the concept of motions in the magnetosphere, but the actual cause of the viscous interaction is not definitely known. There are three main possibilities that could cause viscous interaction:

(a) Turbulent plasma with magnetic field outside the boundary, may have random magnetosonic and

Alfven waves. Axford has shown by using the refraction of sound waves[42] that they can bring the required energy in the magnetosphere to provide effective viscous interaction.

(b) If the magnetospheric boundary were unstable (this does not necessarily mean that large scale motion of the boundary movement is necessary) in respect to small perturbations, the turbulent mixing of the solar wind and magnetospheric boundary could produce viscous interaction. This has been worked out by Parker[43] in detail.

(c) Surface instabilities could cause transport of surface tubes of force giving one form of viscous interaction.

It is not known which effect is responsible entirely for the viscous interaction. Probably several effects together could cause the required viscous interaction. Piddington[44] and Dungey[45] have considered this problem using different methods of approach. The final results in all cases, is circulatory motions in the magnetosphere. Some explanation of Figure 12 is in order. If we take a view looking from the sun, the solar wind flows from the direction we are looking. As proposed by several authors and as evidenced by the recent magnetic field results of the IMP satellite[45], a standing shock is formed at 14 to 16 R_E. It has been proposed that the plasma is thermalized after passing through the shock front(some kinetic energy is

converted into random motion). As the plasma travels inward around the magnetosphere the velocity increases and the flow again becomes supersonic behind the earth. The streamlines of the internal motions are shown by the lines in the magnetosphere. The internal stream lines are also the equipotentials of the electric field set up by the charge accumulations as shown in the Figure 12. An indirect observation of the charge accumulation was obtained by observations of auroral hydrogen emisson[47]. We shall assume in the model for the generation of the transverse hydromagnetic waves in the magnetosphere that such internal motions exist. As discussed previously, geophysical phenomena certainly support such an assumption.

3. Generation of Hydromagnetic Waves Inside the Magnetosphere

We shall consider the model magnetosphere as shown in Figure 12. The stream lines in the magnetospheric equatorial cross-section are the equipotential surfaces and also the velocity of the matter is tangent to these lines. From Appendix B we know that the ionized matter (plasma) in the magnetosphere can be considered as a highly conducting fluid. According to the theory discussed in Section 5 of Chapter I, the lines of magnetic field of the earth are "frozen in" and move with the circulatory motions of the plasma. We can write

$$\frac{\partial \underline{B}}{\partial t} = \nabla \times (\underline{v} \times \underline{B}) \qquad (3.1)$$

In order to study the hydromagnetic waves, we use the theory developed in Chapter II. Along with the above equation (3.1), equations (2.4) to (2.7) in Section 2, of Chapter II give the processes involved in the generation of the hydromagnetic waves. However the medium is not isotropic and modifications due to anisotropic conductivity should be made as discussed in Section 3 of Chapter III. Therefore, we shall apply the theory discussed in Chapter III to the model magnetosphere with internal circulatory motions. The hydromagnetic waves observed in the Chapter IV may be generated by small, local perturbations in the velocity of these motions. The velocity perturbations are small and local so that they do not create instabilities. In order to get some quantitative idea of these processes we go back to theory in Chapter III. We would like to get expressions which relate the velocity changes and the corresponding changes in the magnetic fields.

Consider a typical cross-section of the streamline surfaces in the geomagnetic equator of the earth. (Figure 13) The ambient geomagnetic field is approximately perpendicular to this plane. If we select a coordinate system in which the field $\underline{B}$ (approximately B_θ in the spherical coordinate system) is along the X axis, the velocity $\underline{v}$ and $\underline{B}$ lie in the X Y plane. First consider a typical streamline near 1800 hours local time and x, y, z axes as shown in Figure 13 (a).

The plasma flow around the magnetosphere and consequently the "viscous interaction" give such a velocity

pattern in that hemisphere.

Assume that the small perturbations in the velocity and the magnetic field are

$$\begin{aligned} \underline{v} &= \underline{v}_0 + \underline{v}' \\ \underline{B} &= \underline{B}_0 + \underline{b} \end{aligned} \tag{3.2}$$

The relation between $\underline{v}'$ and $\underline{b}$ can be found by the use of the theory in Chapter III. In that treatment we eliminated $\underline{v}'$. Now we are interested in the relation between $\underline{v}'$ and $\underline{b}$. If we make use of the equations (3.14) to (3.16) of Section 3, Chapter III and the dispersion equation

$$\frac{\omega^2}{k^2} = U_A^2 \left\{ 1 - \frac{\sin^2\theta}{2} \mp \left(\frac{\sin^4\theta}{4} + \frac{\omega^2}{\Omega_i^2} \cos^2\theta \right)^{1/2} \right\} + \frac{i\omega}{\mu\sigma_0} \tag{3.3}$$

neglecting the absorption, we have velocity components of the perturbation velocity $\underline{v}'$. They are given as follows

$$\frac{v_z'}{v_y'} = \cos^2\theta \frac{b_z}{b_y} \tag{3.4}$$

The waves shown in Figures 8 (1) to 8 (4) are on the evening side of the magnetosphere (the symmetry line is not 1200 hours but 1045 hours.) These waves are anticlockwise looking down from the north pole on the magnetosphere[33]. In these waves most of the perturbation is along B_r, i.e., the Z axis in the coordinate system of the Figure 13 (a). If we take $\cos^2\theta \approx 1$ (this is reasonable because the maximum angle considered is 10°), we find that

$$\frac{b_z}{b_y} = \frac{b_r}{b_\phi} \approx \frac{3}{1} \tag{3.5}$$

Therefore,

$$\frac{v'_z}{v'_y} \simeq \frac{3}{1}$$

The plasma oscillates in the form of ellipse with major axis along Z axis. The direction of the rotation is anticlockwise. At extremely low frequencies, only v'_z will have significant value.

Now consider the flow line in the morning side of the magnetosphere. The velocity is such that it is toward increasing west longitude. The ccordinate system considered there is shown in Figure 13 (b). Perturbation in the velocity $\underline{v}$ produces waves which are of opposite direction than those produced in the evening side. v'_y, v'_z and b_y, b_z are related by equation (3.4), but the y axis is reversed in Figure 13 (a) and 13 (b). We apply equation (3.4) to the clockwise waves in the magnetosphere.

Figures 8 (5) to 8 (8) show that the perturbation along b_ϕ direction is larger than that along b_r. We can write approximately that

$$\frac{b_r}{b_\phi} = \frac{1}{4} \qquad (3.6)$$

$$\frac{v'_z}{v'_y} \simeq \frac{1}{4}$$

This ratio varies slightly depending on how far the observations are made from the symmetry line. The velocity perturbation is four times larger along the y axis in Figure 13 (b), and plasma oscillates in the form of an ellipse with the major axis along y axis. (On the evening side the plasma oscillates in the ellipse with major axis

along x axis). At very low frequencies the oscillations of the plasma are mainly along y axis. These clockwise waves in the magnetosphere become anticlockwise on the surface of the earth when viewed from the north pole.

Thus, the model given here explains the main features of the transverse locally produced hydromagnetic waves observed in the outer magnetosphere (7 to 10 R_E).

4. Rotation of the Symmetry Line of the Opposite Polarizations

The study of transverse hydromagnetic waves in Chapter IV shows clearly that the waves have opposite polarization on either side of 1045 hours local time, i.e., approximately 22° from the sun-earth line as shown in Figure 13. We have discussed several other geophysical phenomena such as giant micropulsations[23] and SC perturbations in the geomagnetic storms[22] that show such rotation of the symmetry line. Also the D_s current system[48] and S_q polar current patterns[49] in the ionosphere show similar rotation of the symmetry line.

Wilson attempted to explain this rotation in the case of SC perturbation interpreted as transverse hydromagnetic waves that the shock wave responsible for the SC arrives at an inclination rather than radial. Although this may possibly occur during storms, the quiet day solar plasma flow should be approximately radial[50]. The symmetry line should then be 1200 hours local time.

Axford[40] has suggested that the rotation of the

earth and the magnetosphere with it can cause such a rotation. The model internal motions in the magnetosphere in Figure 12 show that the return flow lines reach the edge of the magnetosphere in the sunward side. If this is so, the viscous interaction, dependent on the relative velocity between the plasma and the magnetosphere, would be at a minimum to the west of the noon meridian. The zero relative velocity position would be shifted west by the rotation of the magnetosphere and the line of symmetry coincident with zero relative velocity would also be shifted. [51] If the return flow lines do not reach the edge of the sunward side, the point 0 would shift in the opposite side, i.e., evening side. This has never been observed in any geophysical phenomena. *

---

* Leinbach has found recently that mid-day recovery of polar cap absorption (PCA) is not exactly 1200 hours local time but shifted to 1100. This is additional support to the westward asymmetry.

CHAPTER VI

SUMMARY

Low frequency hydromagnetic waves have been studied in the outer magnetosphere. A method was devised to separate the transverse hydromagnetic waves and longitudinal magnetosonic waves in data from the Explorer XII satellite flux-gate magnetometer observations.

Several examples of transverse hydromagnetic waves were found in the outer magnetosphere from 7 to 10 earth radii (R_E) equatorial distance. These waves had amplitudes of 10 gammas and periods ranging from 100 to 200 seconds. The waves were circularly or elliptically polarized.

The transverse waves should travel along field lines of the earth's magnetic field and produce corresponding changes in the surface magnetic records. Two examples of this effect were found. The transverse hydromagnetic waves observed by the satellite in the magnetosphere at 8 R_E were found to cause similar effects on the surface magnetic records after 1 1/2 minute delay. The amplitude may have been reduced. Correlation between transverse waves in space and in ground measurements has been found for the first time in this study.

Some examples of magnetosonic waves were also found. They had approximately 10 gammas amplitude and periods of 100 to 200 seconds. Some of the findings of

this work support previous satellite observations which were unfortunately, handicapped by the lack of complete information of the vector magnetic field. This study reveals some new features. Polarizations of the waves can be determined directly in this investigation. Quantitive study of the transverse hydromagnetic waves indicate that

(a) Circular or elliptical polarizations are due to the anisotropic conducting plasma medium in the outer magnetosphere.

(b) The waves have an anticlockwise polarization between 1045 and 1200 hours local time.

(c) The waves have a clockwise polarization between 0700 and 1045 hours local time. These polarization directions are determined for an observer looking down from the north pole.

(d) The symmetry axis of opposite polarizations of these transverse waves is 1045 hours and not 1200 hours local time. Similar rotation of symmetry axis is found in many geophysical phenomena observed on the earth, e.g., giant micropulsations, SC perturbations, D_s current system and quiet time polar S_q current pattern. For the first time evidence is found that such rotation of symmetry axis exists even in the far out magnetospheric region.

Finally, a model was obtained which can explain the above observed properties of the transverse waves in the magnetosphere. This model is based on the "unified model" advanced by Axford and Hines[41] and Axford[40] giving internal

motions in the magnetosphere. The model described here can generate the small scale, short-lived transverse waves inside the magnetosphere and explain the opposite polarizations and the rotation of the symmetry axis. It is also unified with similar phenomena mentioned above.

The importance of quantitive knowledge of hydromagnetic waves can be realized from the above discussion of the associated phenomena. This direct evidence of the propagation of hydromagnetic waves to the surface of the earth and rotation of the symmetry line should help in understanding the theoretical aspects of "micropulsations", D_s, and S_q current systems, and internal motions in the magnetosphere. Definite knowledge of the amplitudes and periods of these waves in the magnetosphere is required to understand the complex processes involved in the determination of the life time of the Van Allen radiation belts. The hydromagnetic waves found here have such period that the third adiabatic invariant could be violated and this could affect the trapped particles in the outer Van Allen belt. A discussion on this topic is out of place here, but survey can be found in a paper by Judge and Coleman[26]. These waves should also provide us knowledge of the properties of the plasma in the magnetosphere as deduced in this study. Some properties of the plasma in the outer magnetosphere are calculated on the present knowledge of N, T, and B to verify these deductions.

BIBLIOGRAPHY

1. H. Alfven and C. G. Falthammar, Cosmical Electrodynamics (Oxford University Press, New York, 1963).

2. J. W. Dungey, Pennsylvania State University Scientific Report No. 69 (1954) (See also Geophysics: The Earth's Environment edited by C. DeWitt, J. Heibolt and A. Lebeau (Gordon and Breach, London, 1963)).

3. M. Sugiura, Phys. Rev. Letters 6, 255 (1961).

4. R. Gallet, Geophysics: The Earth's Environment (Gordon and Breach, London, 1963).

5. H. Alfven, Arkiv. f. Mat 29B, No. 2 (1942).

6. V. C. A. Ferraro and C. Plumpton, Magneto-fluid Mechanics (Clarendon Press, Oxford, 1961)

7. T. G. Cowling, Magnetohydrodynamics p. 5 (Interscience Publishers, Inc., New York, 1957)

8. S. Lundquist, Nature 164, 145 (1949) Also Phys. Rev. 76, 1805 (1949).

9. J. M. Wilcox, A. W. DeSilva, W. S. Cooper, Phys. Fluids 4, 1506 (1961).

10. T. G. Cowling, Magnetohydrodynamics p. 7 (Interscience Publishers, Inc., New York, 1957).

11. J. W. Dungey, Cosmic Electrodynamics (Cambridge University Press, 1958).

12. J. Carstoiu, Proc. Roy. Soc. 46, 131 (1960).

13. V. L. Ginzburg, Propagation of Electromagnetic Waves in Plasma p. 267 (Gordon and Breach Science Publishers, New York, 1960).

14. V. L. Ginzburg, Propagation of Electromagnetic Waves in Plasma p. 291 (Gordon and Breach Science Publishers, New York, 1960)

15. A. Banos, Electromagnetic Phenomena in Cosmical Physics LAU Symposium 6, (Cambridge University Press 1958)

16. T. E. Stringer, Plasma Physics (J. Nucl. Energy, Part C 5 89 (1963)

17. L. D. Landau and E. M. Lifshitz, Electrodynamics of Continuous Media, p. 222 (Addison Wesley Publishing Co., Reading, Mass. 1960)

18. B. Lehnert, Phys. Rev. 94, 815 (1954).

19. W. H. Bostick and M. A. Levin, Phys. Rev. 87, 671 (1952)

20. H. A. Bomke, W. J. Ramm, S. Goldblat and V. Klemas, Nature 185, 299 (1960)

21. H. Maeda and T. Ondoh, Nature, 188, 1018 (1960)

22. C. R. Wilson and M. Sugiura, J. Geophys. Research 66, 4097 (1961)

23. T. Nagata, S. Kokubun and T. Iijima, J. Geophys. Research 68, 4621 (1963)

24. C. P. Sonett, A. R. Sims and I. J. Abrams, J. Geophys. Research 67, 1191 (1962)

25. P. J. Coleman, C. P. Sonett, D. L. Judge and E. J. Smith, J. Geophys. Research 65, 1856 (1960)

26. D. L. Judge and P. J. Coleman, J. Geophys. Research 67, 5071 (1962)

27. J. R. Balsey, Advances in Geophysics 1, 313 (1952)

28. L. J. Cahill, Jr., Space Science Review 1, 399 (1962-1963)

29. L. J. Cahill, Jr., P. G. Amazeen, J. Geophys. Research 68, 1835 (1963)

30. J. H. Piddington, Monthly Notices Roy. Astron. Soc. 114, 638 (1954)

31. C. P. Sonett, J. Geophys. Research 68, 6571 (1963)

32. W. I. Axford, J. Geophys. Research 68, 5883 (1963)

33. V. L. Patel and L. J. Cahill, Jr., Phys. Rev. Letters 12, 213 (1964)

34. L. J. Cahill and V. L. Patel, Transactions AGU 43, 459 (1962)

35. Y. Kato and S. I. Akasofu, Sci. Rept. Tohoku University, Fifth Ser. 7, 103 (1956)

36. T. Watanabe, Sci. Rept. Tohoku University, Fifth Ser. 13, 127 (1961)

37. J. R. Melcher, Phys. Fluids, 4, 1348 (1961)

38. J. A. Fejer, Phys. Fluids, 6, 508 (1963)

39. C. R. Wilson, J. Geophys. Research 67, 2054 (1962)

40. W. I. Axford, Planetary and Space Science, 12, 45 (1964)

41. W. I. Axford and C. O. Hines, Canadian J. Phys. 39, 1433 (1961)

42. H. S. Ribner, J. Acoust. Soc. Amer. 29, 435 (1957)

43. E. N. Parker, Phys. Fluids 1, 171 (1958)

44. J.H. Piddington, Planetary and Space Science 9, 947 (1962)

45. J. W. Dungey, Phys. Rev. Letters 6, 47 (1961)

46. N. F. Ness, IMP 1 Symposium at Goddard Space Flight Center, March 12, 1964

47. W. Stoffregen and H. Derblom, Planetary and Space Science 9, 711 (1962)

48. S. Chapman, Vistas in Astronomy 2, 912 (1956)

49. T. Nagata and K. Kokubun, Nature, 195, 555 (1962)

50. E. N. Parker, Interplanetary Dynamical Processes, p. 139 (Interscience Publishers, John Wiley, New York, 1963)

51. H. Leinbach, Transaction AGU 45, 76 (1964)

52. R. L. Smith, J. Geophys. Research 66, 3709 (1961)

53. K. I. Gingauz, V. G. Kurt, V. I. Moroz, I. S. Shklovskii, Planetary and Space Science 9, 21 (1962)

54. V. L. Ginzburg, Propagation of Electromagnetic Waves in Plasma Chapter II, Section VI, (Gordon and Breach, New York, 1960)

55. B. Lehnert, Nuovo Cemento Suppliments 13, Series X, 76 (1959)

APPENDIX A

GENERALIZED OHM'S LAW AND APPROXIMATIONS FOR $J=\sigma E'$

We wish to derive the conditions in which the simple form of Ohm's law $J=\sigma E'$ holds for the medium such as the electron-ion component plasma in the magnetosphere. First, we shall derive the generalized Ohm's law and then get $\underline{J}=\sigma E'$. Consider the equation of motion for each component as

$$m_i n\left(\frac{\partial \underline{v}_i}{\partial t}+(\underline{v}_i\cdot\nabla)\underline{v}_i\right)=en\left(\underline{E}+\underline{v}_i\times\underline{B}\right)-\nabla p_i+m_i n\nu_{ei}\times(\underline{v}_e-\underline{v}_i)-nm_i\nabla\phi \tag{A.1}$$

$$m_e n\left(\frac{\partial \underline{v}_e}{\partial t}+(\underline{v}_e\cdot\nabla)\underline{v}_e\right)=-en\left(\underline{E}+\underline{v}_e\times\underline{B}\right)-\nabla p_e+m_e n\nu_{ei}(\underline{v}_i-\underline{v}_e)-nm_e\nabla\phi \tag{A.2}$$

where subscripts e and i are for electrons and ions. It is assumed that $n = n_i = n_e$ the pressure $p = nkT$ is a scalar and ϕ is the gravitational potential. ν_{ei} is the electron-ion collision frequency. Define the following quantities:

$$\rho_m=\rho_i+\rho_e\ ;\ \rho_i=n_i m_i\ ;\ \rho_e=n_e m_e$$

$$\underline{v}=\frac{\rho_i\underline{v}_i+\rho_e\underline{v}_e}{\rho_i+\rho_e}\ ;\ p=p_i+p_e\ ;\ \underline{J}=e(n_i\underline{v}_i-n_e\underline{v}_e) \tag{A.3}$$

We shall assume electrical neutrality $n = n_i = n_e$ implying characteristic length

$$L_c \gg L_D \qquad \text{Debye Length} \tag{A.4}$$

Now if we add equations (A.1) and (A.2) we get the equation of motion.

$$\rho_{in}\frac{d\underline{v}}{dt} = \underline{J}\times\underline{B} - \nabla\underline{\underline{p}} - \rho_{in}\nabla\Phi \qquad (A.5)$$

In order to get the generalized Ohm's law, multiply (A.1) by $\frac{e}{m_i}$, and (A.2) by $\frac{e}{m_e}$ and subtract the latter from the former. We get

$$e\left(n\frac{\partial \underline{v}_i}{\partial t} - n\frac{\partial \underline{v}_e}{\partial t}\right) = e\left\{(\underline{v}_e\cdot\nabla)\underline{v}_e - (\underline{v}_i\cdot\nabla)\underline{v}_i\right\} + e^2\left(\frac{n}{m_i}+\frac{n}{m_e}\right)\underline{E}$$
$$+e^2\left(\frac{n\underline{v}_i}{m_i}+\frac{n\underline{v}_e}{m_e}\right)\times\underline{B} - \frac{e}{m_i}\nabla p_i + \frac{e}{m_e}\nabla p_e$$
$$- e\nu_{ei}(\underline{v}_i-\underline{v}_e)\left(\frac{n}{m_i}+\frac{n}{m_e}\right)$$

The gravitation force drops out, considering $m_e \ll m_i$ and $(\underline{v}_e\cdot\nabla)\underline{v}_e \simeq (\underline{v}_i\cdot\nabla)\underline{v}_i$, we get

$$\frac{\partial \underline{J}}{\partial t} = \frac{ne^2\underline{E}}{m_e} - \frac{e}{m_e}\underline{J}\times\underline{B} + \frac{ne^2}{m_e}(\underline{v}_i\times\underline{B}) + \frac{e}{m_e}\nabla p_e - \nu_{ei}\underline{J} \qquad (A.6)$$

This is the generalized Ohm's law. We make the following approximations:

(a) For low frequencies

$$\omega << \Omega_i \qquad (A.7)$$

We have $\underline{v}_i >> \frac{m_e}{m_i}\underline{v}_e$; therefore

$$\underline{v} = \frac{\rho_i\underline{v}_i + \rho_e\underline{v}_e}{\rho_i+\rho_e} \simeq \frac{\rho_e}{\rho_i}\underline{v}_e + \underline{v}_i \simeq \underline{v}_i$$

Using this in (A.6) and dividing through ν_{ei}, we get

$$\frac{1}{\nu_{ei}}\frac{\partial \underline{J}}{\partial t} + \underline{J} + \frac{\omega_e}{\nu_{ei}}\left(\frac{\underline{J}\times\underline{B}}{B}\right) = \frac{ne^2}{m_e\nu_{ei}}\left(\underline{E}+\underline{v}\times\underline{B}\right) \qquad (A.8)$$

where $\omega_e = \frac{eB}{m_e}$

(b) With the approximations

$$\omega << \nu_{ei}$$
$$\omega_e << \nu_{ei} \qquad (A.9)$$

We consider changes $J = J_o e^{i\omega t}$ and taking ν_{ei} as ν_{eff} in equation (A.8), we get

$$\underline{J} = \frac{ne^2}{m_e \nu_{eff}} \left(\underline{E} + \underline{v} \times \underline{B} \right) \tag{A.10}$$

Therefore, with $\sigma = \frac{ne^2}{m_e \nu_{eff}}$ and $\underline{E}' = \underline{E} + \underline{v} \times \underline{B}$ we have

$$\underline{J} = \sigma \underline{E}' \tag{A.11}$$

This simple form of Ohm's law is valid in a two-component electron-ion plasma in most cases with approximations (A.7) and (A.9). They are called hydromagnetic approximations and therefore sometimes (A.11) is also referred to as the hydromagnetic approximation.

APPENDIX B

PLASMA PARAMETERS IN THE MAGNETOSPHERE

In order to apply plasmadynamics in the magnetosphere, we should have knowledge of the several papameters. This will enable us to see whether the approximations made in considering the medium in the magnetosphere as plasma is acceptable or not. Recently, some doubts have been expressed whether the medium in the magnetosphere should be considered as a conductor or a dielectric[1]. We wish to check this and to show that the medium from 6 to 10 earth radii is highly conducting (this may not be true at less than 3 earth radii). Also, we shall show that this conducting medium is not isotropic as assumed before, but is anisotropic. In order to do these calculations we should know the plasma density N, the temperature T and the magnetic flux density B. The knowledge of these quantities is scanty, but we can take reasonable estimates of these quantities from satellite measurements. The uncertain values of these quantities may cause slight errors in the values of the parameters computed, but still we can get an idea of the order of the magnitude of the parameters. Table 3 gives the values of N, T and B and shows the source of this information.

TABLE 3

VALUES OF CERTAIN QUANTITIES IN THE MAGNETOSPHERE

QUANTITY	VALUE	SOURCE
N	50×10^6 #/m^3	Whistlers, Space Rocket[52]
T	10^4 °K	Soviet Space Rocket [53]
B	100-200 γ	Explorer XII[29]

Using the value of 200 γ, for the magnetic field, the Larmor frequencies of electrons and ions, ω_e and Ω_i are calculated. We are interested in waves of 100 to 200 seconds period. The wave frequency ω, and ω_e, Ω_i are tabulated in Table 4.

TABLE 4

LARMOR AND WAVE FREQUENCIES

FREQUENCY	RAD/SEC	PERIOD	SEC
Ω_i	20	T_i	0.33
ω_e	4×10^4	T_e	1.8×10^{-4}
ω	$3\text{-}6 \times 10^{-2}$	T_{wave}	100 - 200

From Table 3, taking values of N, T and B, we calculate the Debye length L_D, velocities of electrons and protons $(V_T)_e$ and $(V_T)_i$ with temperature 10^4 °K, Larmor radii R_e and R_i with B=200 γ. The values of all these quantities are given in Table 5.

TABLE 5

NUMERICAL VALUES OF CERTAIN PARAMETERS DEPENDENT ON N, T, B.

QUANTITY	FORMULA	VALUE
L_D	$\left(\frac{kT\epsilon_0}{2Ne^2}\right)^{1/2}$	1m
$(V_T)_e$	$\left(\frac{kT}{m_e}\right)^{1/2}$	10^5 m/sec
$(V_T)_i$	$\left(\frac{kT}{m_i}\right)^{1/2}$	10^4 m/sec
R_e	$\frac{m_e V}{Be}$	16 m
R_i	$\frac{m_i V}{Be}$	500 m
ω_p	$\left(\frac{N_e e^2}{m_e \epsilon_0}\right)^{1/2}$	4×10^5 rad/sec

Now we wish to compute the conductivity of the medium. We should first know the collision frequencies of electron and ion. In elementary theory, the effective collision frequency of an electron is given by

$$\nu_{eff} = \pi a^2 N \bar{v} \qquad \text{(B.1)}$$

where a is the radius of the molecule or atom and N, the number of molecules in unit volume and $\bar{v}$ is the average velocity of the electron. In this formula it is assumed that cross-section does not depend on the velocity of the electron. The particles are considered neutral.

We shall consider a more exact treatment of the collision frequency. First, consider the electrons making collisions with ions, neutral molecules and electrons. All these collisions contribute to the conductivity due to electrons. On the same basis collisions of ions with other particles can contribute to the conductivity (usually this is small). The effective electron collision frequency ν_{eff}^{e} is made of three parts:

$$\nu_{eff}^{e} = \nu_{eff;i}^{e} + \nu_{eff;e}^{e} + \nu_{eff;m}^{e} \qquad (B.2)$$

However, $\nu_{eff,e}^{e}$, collision frequency of electron-electron is negligible and we calculate $\nu_{eff,i}^{e}$ and $\nu_{eff,m}^{e}$. In these calculations, we use the kinetic theory.[54] The application of kinetic theory to plasma requires that

$$\frac{\omega_p^2}{\omega^2} \gg 1$$

where ω_p is the plasma frequency. This condition is valid in our treatment (see Table 6). The general procedure is to solve the Boltzmann equation and get the change in distribution function due to collisions and obtain an expression for the current, and hence the conductivity. The whole procedure has been derived but not given here. The expression for the conductivity is compared to the one derived from elementary theory i.e.

$$\sigma = \frac{N_e e^2 \nu_{eff}^{e}}{(\omega^2 + \nu_{eff}^{e2})} \qquad (B.3)$$

(This is due to electron collisions, a similar part should be added for ion collisions replacing ν_{eff}^{e} by ν_{eff}^{i}).

In general, if ν_{eff} were a function of $\underline{v}$ and ω, σ is multivalued. But we can assume ν_{eff} is a function of $\underline{v}$ only and independent of ω. This is justified if

$$\omega \gg \nu_{eff} \tag{B.4}$$

This condition is weakly satisfied in our problem, but it cannot make a difference of more than 1/2 and certainly will not change the order of magnitude of the value of ν_{eff} calculated. The general expression for the effective electron collision frequency for one kind of collision is obtained by comparing the expression for the current density from kinetic theory and equation (B.5) with equation (B.4).

$$\nu_{eff}^{e} = \frac{2}{3\pi^{1/2}} \left(\frac{m_e}{kT}\right)^{5/2} \int_0^{\infty} \nu(v)\, v^4\, e^{-\frac{mv^2}{2kT}}\, dv \tag{B.5}$$

where $\nu(v)$ is the collision frequency obtained from the cross-section for a particular collision and other symbols have usual meaning. We evaluate $\nu_{eff,i}^{e}$ and $\nu_{eff,m}^{e}$ from (B.5) and write for convenience ν_{ei} and ν_{em} respectively.

(1) Calculation of ν_{ei}

First find $\nu(v)$ for electron-ion collision and use it in (B.5), and replace ν_{eff}^{e} by ν_{ei} . We have an expression for electron-ion collision frequency as

$$\nu_i(v) = \frac{\bar{v}_e}{l} = v_e N_i q_i \qquad \text{(B.6)}$$

where q_i is the transport cross-section for the electron-ion collision, l is the mean free path of the electron. The transport cross section is obtained by $\int q(v,\theta)(1-\cos\theta)\, d\Omega$. The factor $(1-\cos\theta)$ allows the appropriate effects (scattering angle θ large or small). In this case we can use Rutherford cross-section and evaluate q_i by approximating at distance of Debye length L_D. We get ν_{ei} by integration of (B.5).

$$\nu_{ei} = \frac{2\pi}{3}\left(\frac{e^2}{kT}\right)^2 \frac{N_i \bar{v}}{16\pi\epsilon_0^2} \ln\left\{\frac{2kT L_D (4\pi\epsilon_0)}{(1.78)e^2}\right\} \qquad \text{(B.7)}$$

After numerical computation, we get

$$\nu_{ei} = 3.3\times10^{6}\frac{N_i}{T^{3/2}} \ln\left\{2.3\times10^{5}\left(\frac{T}{N_i^{1/3}}\right)^{3/2}\right\} \qquad \text{(B.8)}$$

(2) Calculation of ν_{em}

If we use $\nu(v)$ for electron-neutral molecules we can find ν_{em} from (B.5). In these collisions with molecules, long range Coulomb forces are not involved and the cross-section weakly depends on v and θ. Therefore we can take cross-section $q_m = \pi a^2$ where a is the radius of molecules or atoms (10^{-10}m). The collision frequency of electron and neutral atom is given by

$$\nu_m = v_e N_m q_m \qquad \text{(B.9)}$$

Evaluating (B.5) with (B.9) we get an effective ν_{em} as

$$\nu_{em} = \frac{4\pi}{3} a^2 N_m \bar{v}_e \qquad \text{(B.10)}$$

where $v_e = \left(\frac{8kT}{\pi m_e}\right)^{1/2}$ and N_m is the number of neutral atoms per cubic meter. With numerical calculations, we get

$$\nu_{em} = 2.5 \times 10^{-16} T^{1/2} N_m \qquad \text{(B.11)}$$

Since ν_{ee} is not important (it cannot be neglected however, is $\omega^2 \ll \nu_{eff}^2$) we get total effective collision frequency of electrons with all other particles as

$$\nu_{eff}^{e} = \nu_{ei} + \nu_{em} \qquad \text{(B.12)}$$

With a similar argument, we can calculate collision frequencies of the ions with electrons, ions and ions and ions and neutral molecules or atoms. We shall use the symbol ν_{ii} for effective collision frequency of ions and ions instead of $\nu_{eff;i}^{i}$ and the similar notation for other collisions.

(3) Calculation of ν_{ii}

Ion-ion collision frequency can be obtained from ν_{ei}. Replace v_e by v_i in (B.5). Since both particles are ions

$$v_i = \left(\frac{8kT}{\pi m_i/2}\right)^{1/2}$$

Replace v_e by $3.18 \times 10^{-2}\, v_e$ in equation (B.5) and (B.6). We get

$$\nu_{ii} = 10.4 \times 10^{-8} N_i \ln \left\{ 2.3 \times 10^{5} \left(\frac{T}{N_i^{1/3}}\right)^{3/2} \right\} \qquad \text{(B.13)}$$

(4) Calculation of ν_{im}

Ion-neutral molecules collision frequencies (only neutral hydrogen is important in the outer magnetosphere) can be obtained from ν_{em} by multiplying 3.18×10^{-2} with (B.11)

$$\nu_{em} = 8 \times 10^{-18} T^{\frac{1}{2}} N_m \qquad \text{(B.14)}$$

(5) Calculation of ν_{ie}

Collision frequency of the ions with electrons is obtained simply from

$$\nu_{ie} = \frac{N_e}{N_i} \nu_{ei} \ . \qquad \text{(B.15)}$$

Since $N_e = N_i$, we have $\nu_{ei} = \nu_{ie}$.

Now the effective collision frequency for ions due to all collisions is sum of the collision frequencies of ions and ions and electrons and ions and neutral atoms. All these collision frequencies are tabulated in Table 6 assuming the values of N and ($N_i = N_e = N_m$) and T from the Table 3.

TABLE 6

COLLISION FREQUENCIES IN THE OUTER MAGNETOSPHERE

EFFECTIVE FREQUENCY (ELECTRON)	SEC^{-1}	EFFECTIVE FREQUENCY (ION)	SEC^{-1}
ν_{ei}	10^{-3}	ν_{ie}	10^{-3}
ν_{em}	10^{-6}	ν_{im}	10^{-8}
		ν_{ii}	10^{-5}

From the Table 5, we know that the total effective electron ion collision frequency is approximately that of electron-ion only i.e.

$$\nu_{eff}^{e} = \nu_{ei}$$

Now we have all the necessary information to know the properties of the medium in the magnetosphere. In particular, we want to know about the conductivity of the medium which determines the polarization of the hydromagnetic waves. It is very complicated to determine the conductivity in an ion-electron and neutral molecule medium. The condition which allows treatment of the medium as a plasma (conducting medium) is that the mean free path of an electron should be less than or equal to the characteristic length L_c. In the magnetosphere the mean free path $\ell = 10^8$m and $L_c = 5 \times 10^7$m (8 earth radii). Therefore

$$\ell \simeq L_c \qquad \text{(B.16)}$$

The medium is called "medium density Plasma", therefore the assumption of high conductivity and a fluid description of the plasma in the magnetosphere is valid (see Reference 1, p. 169).

We can neglect the presence of neutral hydrogen atoms in this part of the magnetosphere. In this region

$$N_i = N_e \simeq N_m$$

In order to justify this assumption, we should check that the coupling between the plasma and neutral atoms is weak. It means that there should be very few collisions between plasma and neutral atoms in one wave period. Lehnert[55] gave the following condition for a weak coupling

$$\omega \left(\nu_{in} + \frac{m_e}{m_i} \nu_{en} \right)^{-1} >> 1 \qquad \text{(B.17)}$$

Using the values from Tables 3 and 6 we get the values of above expression equal to 10^8. Therefore we consider the medium of the magnetosphere an electron-ion plasma (Plasma flow is not affected by neutral hydrogen atoms.) Now the calculation of the conductivity becomes simple and can be determined from the generalized Ohm's law

$$\underline{J} = \sigma_0 E_{\parallel} + \sigma_1 E_{\perp} + \sigma_2 \frac{\underline{B} \times \underline{E}_{\perp}}{|\underline{E}|} \qquad \text{(B.18)}$$

where σ_0 is the direct conductivity (parallel to B), σ_1 is the Pederson conductivity and σ_2 is the Hall conductivity.

From Appendix A, we know that the medium is isotropic, i.e. σ is the same in all directions, only if

$$\omega_e << \nu_{eff} \approx \nu_{ei}$$

However, the values from Tables 3 and 5 show that this condition is not satisfied. The medium density plasma is usually anisotropic. Since the conductivity due to ion is small, we use the following formulas to compute

conductivities.

$$\sigma_0 = \frac{Ne^2}{m_e \nu_{ei}}$$

$$\sigma_1 = \sigma_0 \left\{ 1 + \frac{1}{\left(\frac{\omega_e}{\nu_{ei}}\right)^2} \right\} \qquad \text{(B.19)}$$

$$\sigma_2 = \sigma_0 \left\{ \frac{\omega_e / \nu_{ei}}{1 + (\omega_e / \nu_{ei})^2} \right\}$$

The values of the conductivities are given in Table 7.

TABLE 7

CONDUCTIVITY OF THE PLASMA IN THE OUTER MAGNETOSPHERE

CONDUCTIVITY	$(\text{ohm-m})^{-1}$
σ_0	1.3×10^{3}
σ_1	$\times 10^{-11}$
σ_2	$\times 10^{-4}$

The values of σ_1, and σ_2, are small compared to σ_0. But the important factor which determines the polarization of the hydromagnetic waves is the ratio $\frac{\sigma_2}{\sigma_1}$. (See p. 42) This ratio has value 10^7 and therefore elliptic polarization is expected for hydromagnetic waves propagating at small angle with the magnetic field directions. This is because whenever there is a perturbation along one axis a significant Hall current flows and adds a small magnetic perturbation in the perpendicular direction. In other words from Chapter III (p. 44) when $\frac{\Omega_i}{\omega} \sim 10^3$, the waves propagating within 10° of the field line are highly elliptically polarized.

After discussing and computing several plasma parameters in the magnetosphere, we give a table of

several ratios the values of which must be known in many assumptions. These ratios are given in Table 8.

TABLE 8

SOME USEFUL DIMENSIONLESS RATIOS

$\frac{\omega}{\Omega_i}$	10^{-3}
$\frac{\omega_e}{\nu_{ei}}$	10^{7}
$\frac{\omega_p^2}{\omega^2}$	10^{12}
$\frac{\omega_p}{\omega_e}$	10
$\frac{\omega_p^2}{\omega_e \Omega_i}$	10^{5}
$\frac{\omega_e \Omega_i}{\omega^2}$	10^{9}
$\frac{4\pi N L_D^3}{Z}$	10^{8}
$\frac{R_e}{L_D}$	16
$\frac{\sigma_2}{\sigma_1}$	10^{7}

We have calculated the parameters usually needed in plasma physics of the magnetosphere. These values from various tables may not be exact since the values of N, T and B are subject to change depending on the geophysical and solar events. But they represent the typical values one might expect on the average and should

certainly give some idea about the medium. However all these computations and conclusions are derived for hydromagnetic waves of period 100 - 200 seconds and some of the conclusions may not be valid for waves of longer or shorter period.

APPENDIX C

HYDROMAGNETIC WAVES AS A LOW FREQUENCY LIMIT OF THE ELECTROMAGNETIC WAVES

We have shown in Chapter II that hydromagnetic waves can be regarded as the vibrations of material lines from the "frozen-in" field concept. There the changes in the magnetic field were obtained. We wish to connect hydromagnetic waves with electromagnetic waves. We should consider the electric field through the wave equation. This is done as follows:

Consider the two Maxwell equations

$$\nabla \times \underline{E} = -\frac{\partial \underline{B}}{\partial t} \tag{C.1}$$

$$\nabla \times \underline{B} = \mu \underline{J} + \mu \epsilon \frac{\partial \underline{E}}{\partial t} \tag{C.2}$$

Taking the curl of (C.1) and using (C.2),

$$\nabla^2 \underline{E} = \mu \frac{\partial \underline{J}}{\partial t} + \mu \epsilon \frac{\partial^2 \underline{E}}{\partial t^2} \tag{C.3}$$

The only term in the above expression not containing E is $\frac{\partial J}{\partial t}$. Its equivalent expression is obtained from Ohm's law with the approximation $\sigma \to \infty$ in Chapter I, Section 3. There we had

$$\underline{E}' = 0 = \underline{E} + \underline{v} \times \underline{B} \tag{C.4}$$

Taking the partial derivative of equation (C.4)

$$\frac{\partial \underline{E}}{\partial t} = -\frac{\partial \underline{v}}{\partial t} \times \underline{B}_0 = -\frac{\rho_m}{\rho_m} \frac{\partial \underline{v}}{\partial t} \times \underline{B} \tag{C.5}$$

The value of $\rho_m \frac{\partial \underline{v}}{\partial t}$ is obtained by adding the equations (A.1) and (A.2) in Appendix A; they give

$$\rho_m \frac{\partial \underline{v}}{\partial t} = -\nabla p + \underline{J} \times \underline{B}_o - \rho_m \nabla \phi$$

Neglecting $-\nabla p$ and $\nabla \phi$, with equation (C.5) we have

$$\frac{\partial \underline{E}}{\partial t} = -\frac{1}{\rho_m} (\underline{J} \times \underline{B}_o) \times \underline{B}_o = \frac{B_o^2}{\rho_m} \underline{J} - (\underline{B}_o \cdot \underline{J}) \frac{\underline{B}_o}{\rho_m}$$

with $\underline{B}_o \cdot \underline{J} = 0$,

$$\frac{\partial \underline{E}}{\partial t} = \frac{B_o^2}{\rho_m} \underline{J}$$

$$\frac{\partial^2 \underline{E}}{\partial t^2} = \frac{B_o^2}{\rho_m} \frac{\partial \underline{J}}{\partial t}$$

Using this expression in equation (C.3) we have

$$\nabla^2 \cdot E = \left(\frac{\mu \rho_m}{B_o^2} + \frac{K_e K_m}{c^2} \right) \frac{\partial^2 \underline{E}}{\partial t^2}$$

$$= \frac{1}{c^2} \left(\frac{c^2 \mu \rho_m}{B_o^2} + K_e K_m \right) \frac{\partial^2 \underline{E}}{\partial t^2}$$

where K_e is diectric constant, $\epsilon = K_e \epsilon_o$, $\mu = K_m \mu_o$ and $C^2 = (\mu_o \epsilon_o)^{-1}$.

The phase velocity is $U_A = C\,(K)^{-1/2}$ where dielectric constant $K = K_e K_m + \frac{C^2 \mu \rho_m}{B^2}$.

This is the low frequency dielectric constant. Usually, $K \gg K_e K_m$, therefore

$$U_A = \frac{B_o}{\sqrt{\mu \rho_m}}$$

This shows that Alfven waves are electromagnetic waves propagating in the plasma with magnetic field in the low frequency limit.

APPENDIX D

PRINCIPLES OF THE FLUX-GATE MAGNETOMETER

The flux-gate magnetometer consists of a core of easily saturable ferromagnetic material of a very high permeability (u) with an external winding. When an A.C. voltage is applied to the winding it produces a magnetic field

$$h = h_o \cos \omega t \qquad \text{(D.1)}$$

as shown in Figure D.1. This varying magnetic field drives the core through the B - H cycle and into saturation as shown in Figure D.2.

Now consider that we have some external field H_o; the total field is

$$H(t) = H_o + h_o \cos \omega t \qquad \text{(D.2)}$$

This total field H decreases during one half cycle and increase during another half cycle. The external field along the core keeps the core saturated along one direction of the driving field, h (t), longer than the other. (See Figure D.3). Because of this the induced EMF in a secondary coil will be distorted (see Figure D.4) and will have an asymmetrical wave having even and odd harmonics of the driving frequency. These odd and even harmonics are the functions of the external field H_o, but only even harmonics are sensitive to its sign and

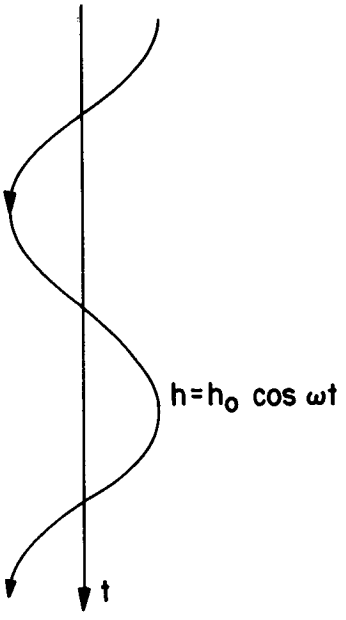
h=h₀ cos ωt
t

(D 1)

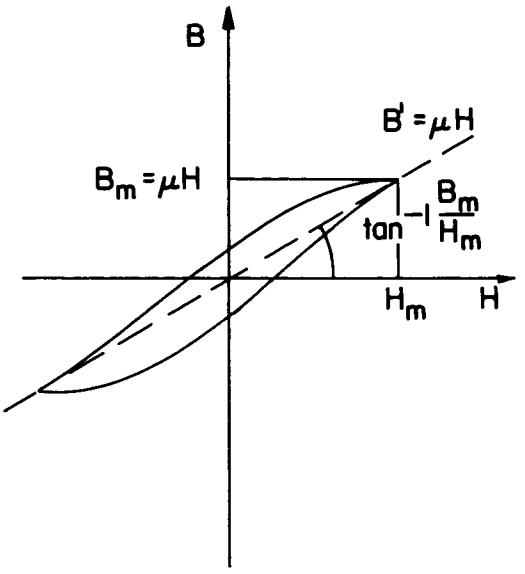
B
B' = μH
Bm = μH
tan⁻¹ Bm/Hm
Hm
H

(D 2)

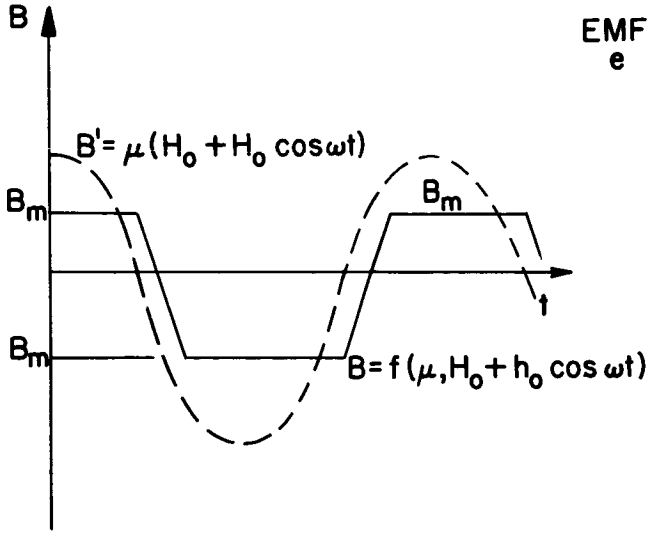
B
B'= μ(H₀ + H₀ cosωt)
Bm
Bm
t
Bm
B= f (μ, H₀+ h₀ cos ωt)

(D 3)

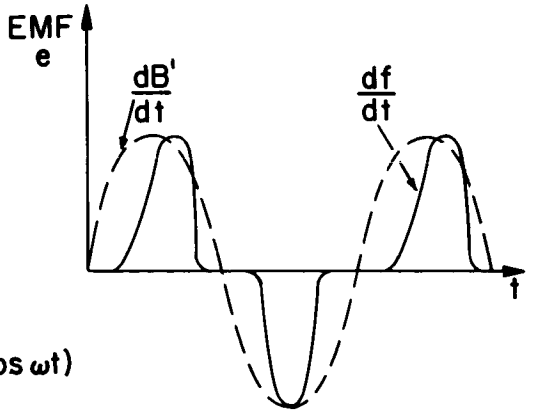
EMF
e
dB'/dt
df/dt
t

(D 4)

vanish when H_o vanishes. Measurement of the amplitude of one or more even harmonics of the output EMF provides a means of measuring the external field along the core.

Two basic methods are used to make such measurements. If we use all even harmonics we have the advantage of using more available energy but the electronics is complicated. The method of using only one even harmonic means less energy is available but there is the advantage of a less complex electronic circuit.

Two problems are inherent in the flux gate magnetometer. The signal voltage corresponding to zero magnetic field may change ("drift") after calibration. Then relative measurements, changes in the magnetic field component are possible but the absolute value is as uncertain as the knowledge at the zero field signal voltage. Drift is caused by temperature changes, supply voltage changes and aging. A second problem is easier to correct and to detect in satellite use than the first. These problems have been considered in the experiment from which the results discussed in Chapter III were obtained.

APPENDIX E

TRANSFORMATION OF THE VECTOR MAGNETIC FIELD FROM THE B, α, ψ COORDINATE SYSTEM TO THE GEOCENTRIC SPHERICAL COORDINATE SYSTEM

The measurement of magnetic field is obtained from the satellite data as B, α, ψ, the field magnitude and the spacecraft direction angles. We are interested in obtaining the components of the magnetic field B_r, B_θ, B_ϕ in the geocentric spherical coordinate system. The following method was followed to achieve this transformation:

(a) First find the Right Ascension α_B and Declination δ_B of the magnetic field vector $\underline{B}$.

(b) From this find the Azimuth A_B and Elevation E_B of the magnetic field vector at the subsatellite point on the earth.

(c) Use these to obtain B_r, B_θ, B_ϕ

Consider the celestial sphere shown in Figure 5. All the pertinent information is represented on that sphere:

1) Right Ascension α_S and Declination δ_S of the spin axis of the satellite are represented by Z on the sphere.

2) Right Ascension α_H and Declination δ_H of the sun are represented by point H. These may be obtained from the American Ephemeris and Nautical Almanac. They were computed here in a routine IBM 1620 program for better accuracy

at any given day and time.

3) P is the celestial north pole, MM' is the celestial equator, $L\gamma L\gamma'$ is the ecliptic, the sun's apparent path on the celestial equator. Π is the north ecliptic pole, γ is the vernal equniox (March 21), and γ' (September 21) the autumnal equinox.

4) B denotes the projection of the magnetic field vector on the sphere. We would like to know

γN = Rt. Ascn. of the field vector = α_B

NB = Declination of the field vector = δ_B (E.1)

5) The experimentally calculated angles α_{Exp} and ψ are indicated on the sphere as:

$$BZH = BZP + PZH = \psi$$
$$ZB = \alpha_{Exp} \qquad \text{(E.2)}$$

a) Calculation of α_B and ψ_B

In order to obtain values of α_B and ψ_B, first consider the spherical triangle PZH in Figure 5. We shall use two formulas from spherical trigonometry.

$$\cos ZH = \sin\delta_S \sin\delta_H + \cos\delta_S \cos\delta_H \cos(\alpha_S - \alpha_H) \qquad \text{(E.3)}$$

Since, α_H, δ_H, α_S, δ_S are known, we calculate ZH. Now use ZH to find angle PZH

$$\cos PZH = \frac{\cos\delta_H \sin(\alpha_H - \alpha_S)}{\sin ZH} \qquad \text{(E.4)}$$

Also, from the sine law for a spherical triangle

$$\operatorname{Sin} PZH = \frac{\operatorname{Cos}\delta_H \operatorname{Sin}(\alpha_H - \alpha_s)}{\operatorname{Sin} ZH} \qquad \text{(E.5)}$$

From equations (E.4) and (E.5) we compute PZH. Using equation (E.2) by knowledge of ψ, we have

$$BZP = \psi - PZH \qquad \text{(E.6)}$$

Now, we have all the necessary information to calculate α_B, δ_B from the spherical triangle PBZ as follows:

1. Calculation of δ_B

   From triangle PBZ, we have

$$\operatorname{Sin}\delta_B = \operatorname{Cos}\alpha \operatorname{Sin}\delta_s + \operatorname{Sin}\alpha \operatorname{Cos}\delta_s \operatorname{Cos} BZP \qquad \text{(E.7)}$$

2. Calculation of α_B

   We want actually γN in Figure 5

$$\gamma N = \alpha_s - NQ \qquad \text{(E.8)}$$

We can calculate NQ which is the same as angle NPQ, from the spherical triangle PBZ.

From the sine law,

$$\frac{\operatorname{Sin} NPQ}{\operatorname{Sin}\alpha} = \frac{\operatorname{Sin} PZB}{\operatorname{Sin}(\pi/2 - \delta_B)}$$

or,

$$\text{Sin NPQ} = \frac{\operatorname{Sin}\alpha \operatorname{Sin} PZB}{\operatorname{Cos}\delta_B} \qquad \text{(E.9)}$$

Also,

$$\text{Cos NPQ} = \frac{\operatorname{Cos}\alpha - \operatorname{Sin}\delta_B \operatorname{Sin}\delta_s}{\operatorname{Cos}\delta_B \operatorname{Cos}\delta_s} \qquad \text{(E.10)}$$

Therefore, we have the Declination of the field vector δ_B from (E.7) and α_B Right Ascension of the field from (E.8) with (E.9) and (E.10).

b) Calculation of the Azimuth A_E and Elevation E_B of the field vector at the subsatellite point translated to the earth.

We know the longitude and latitude of the satellite position at any time. From Figure 6 we can find the azimuth A_B and the elevation E_B of the field vector. In order to do this we should know t_B, the hour angle of the field vector. The field hour angle is given by

$$t_B = \alpha_B - \text{hour angle of the vernal equinox} - \text{longitude of satellite.} \qquad \text{(E.11)}$$

The hour angle of the vernal equinox is available for any day and time from a program prepared for IBM 1620, so we can find t_B. From the spherical triangle KPB,

$$\sin E_B = \sin\theta \sin\delta_B + \cos\theta \cos\delta_B \cos t_B \qquad \text{(E.12)}$$

$$\sin A_B = \frac{\cos\delta_B \cos E_B}{\sin t_B} \qquad \text{(E.13)}$$

c) Calculation of B_r, B_θ, B_ϕ.

Now we can calculate components of the magnetic field vector in geocentric spherical coordinate system from the values of B, α, ψ.

We have,

$$B^2 = B_r^2 + B_\theta^2 + B_\phi^2 \tag{E.14}$$

$$\tan A_B = \frac{B\phi}{B_\theta} \tag{E.15}$$

$$\tan E_B = \frac{-B_r}{(B_\theta^2 + B_\phi^2)^{1/2}} \tag{E.16}$$

where B_r is along the radius vector toward the earth's center, B_θ up and B_ϕ eastward. Since we know B, A_B, E_B we have these equations:

$$B_r = -B \sin E_B \tag{E.17}$$

$$B_\theta = B \cos A_B \cos E_B \tag{E.18}$$

$$B_\phi = B_\theta \tan A_B \tag{E.19}$$

Thus, we have B_r, B_θ, and B_ϕ from the above equations.

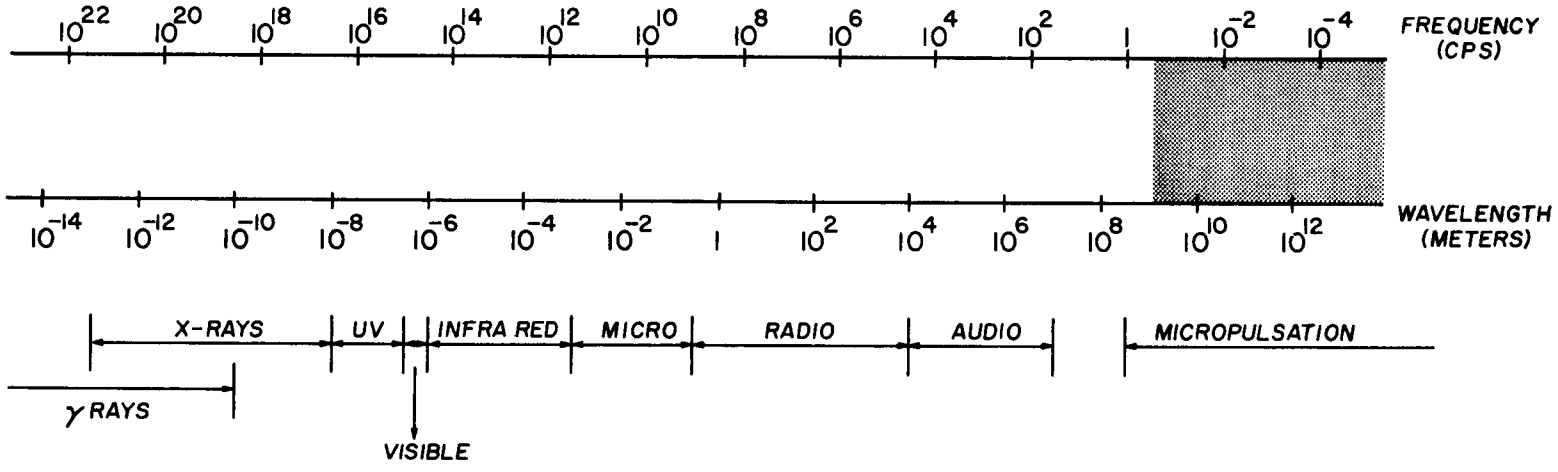

Spectrum of electromagnetic waves (log scale), (after J.R. Heirtzler). The shaded part of very low frequency is of interest here.

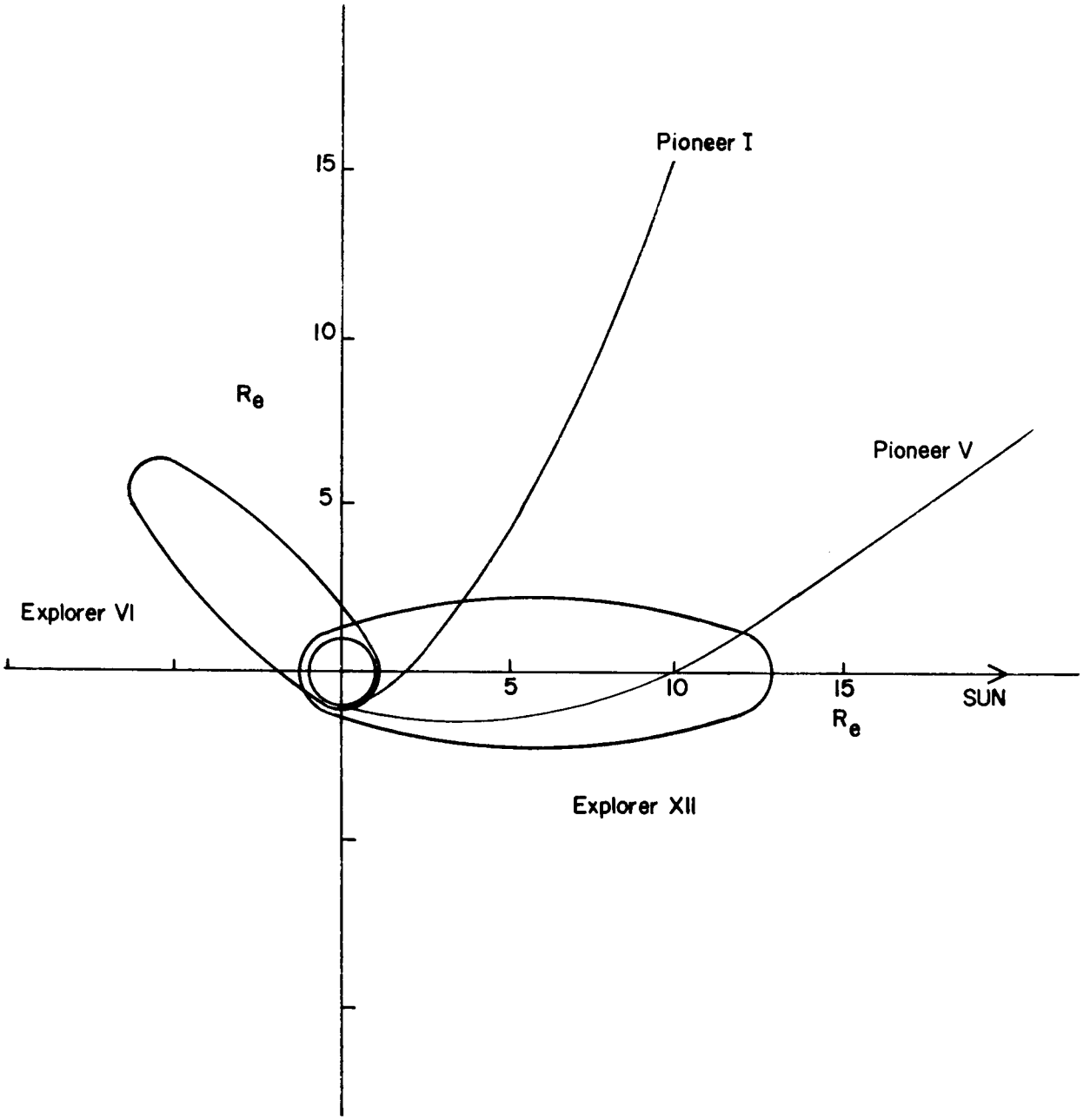
Pioneer I
15
10
R_e
Pioneer V
5
Explorer VI
5
10
15
SUN
R_e
Explorer XII

FIGURE 2

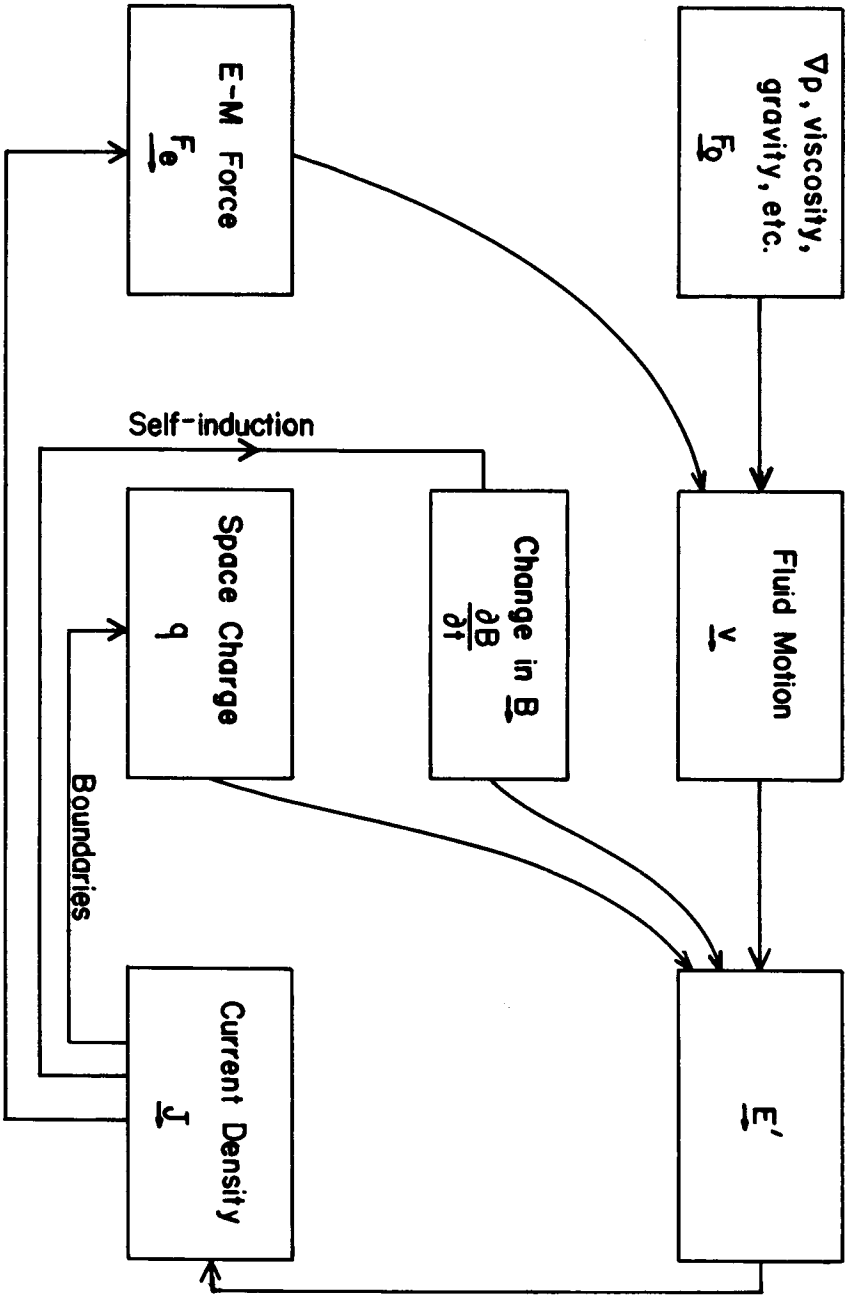
∇p, viscosity, gravity, etc.
F_g
E-M Force
F_e
Fluid Motion
v
Change in B
∂B/∂t
Space Charge
q
Self-induction
Boundaries
Current Density
J
E'

FIGURE 3

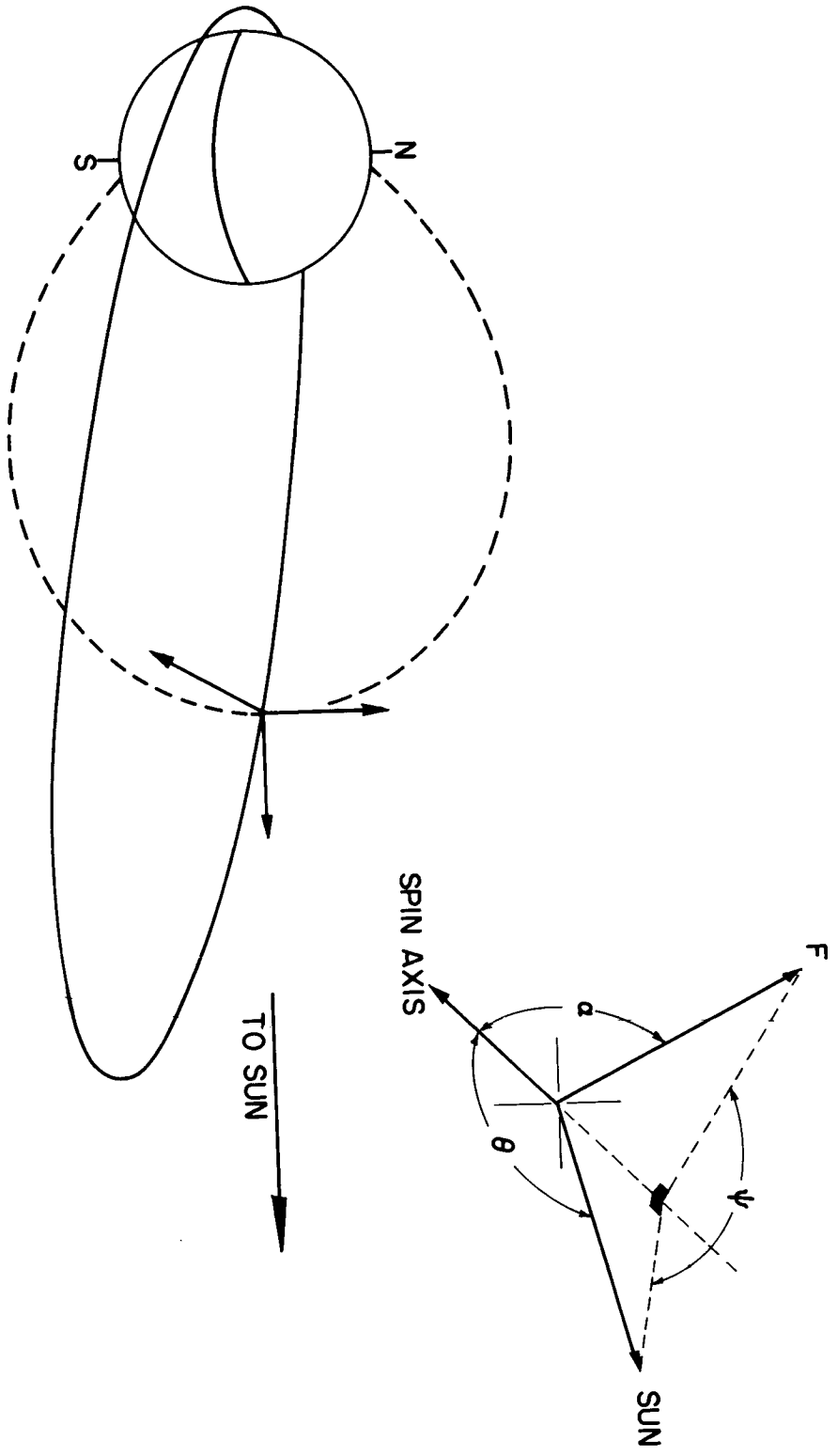

FIGURE 4

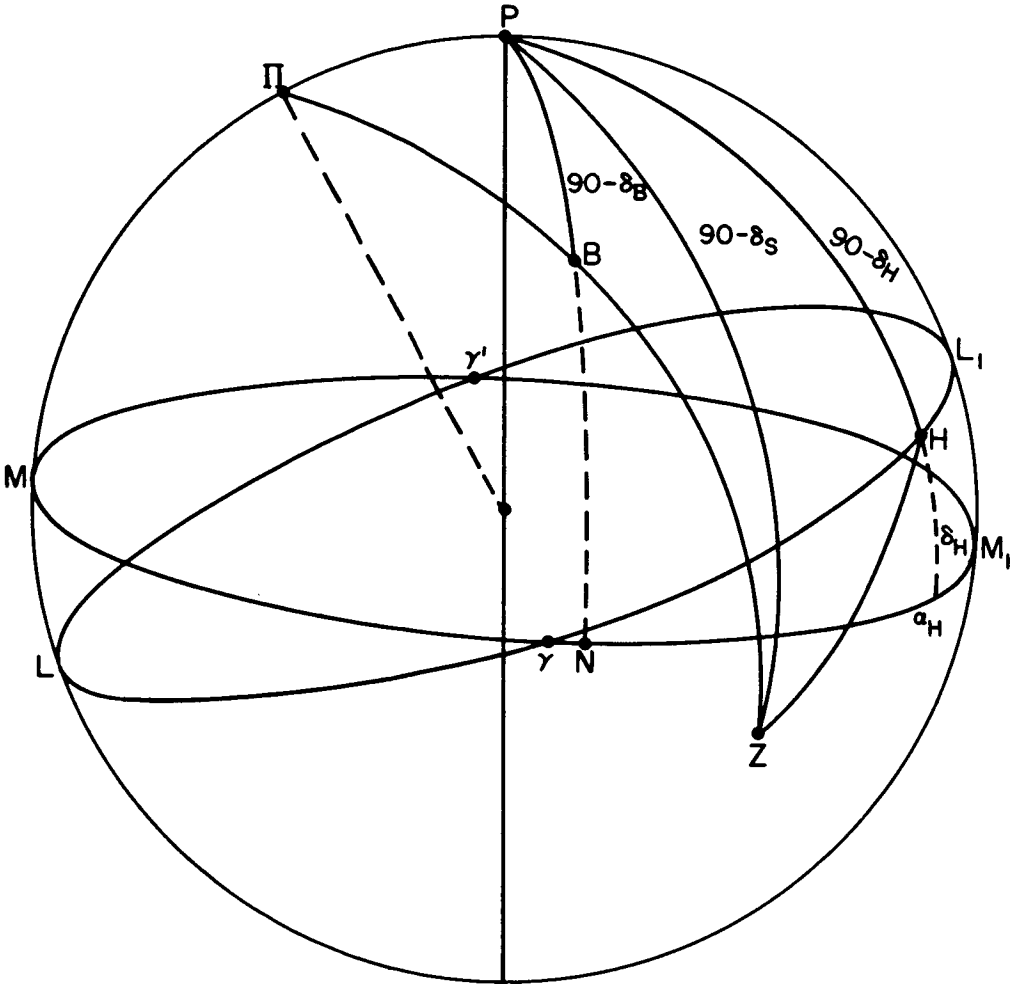

ZB = α experiment
BZP + PZH = ψ

FIGURE 5

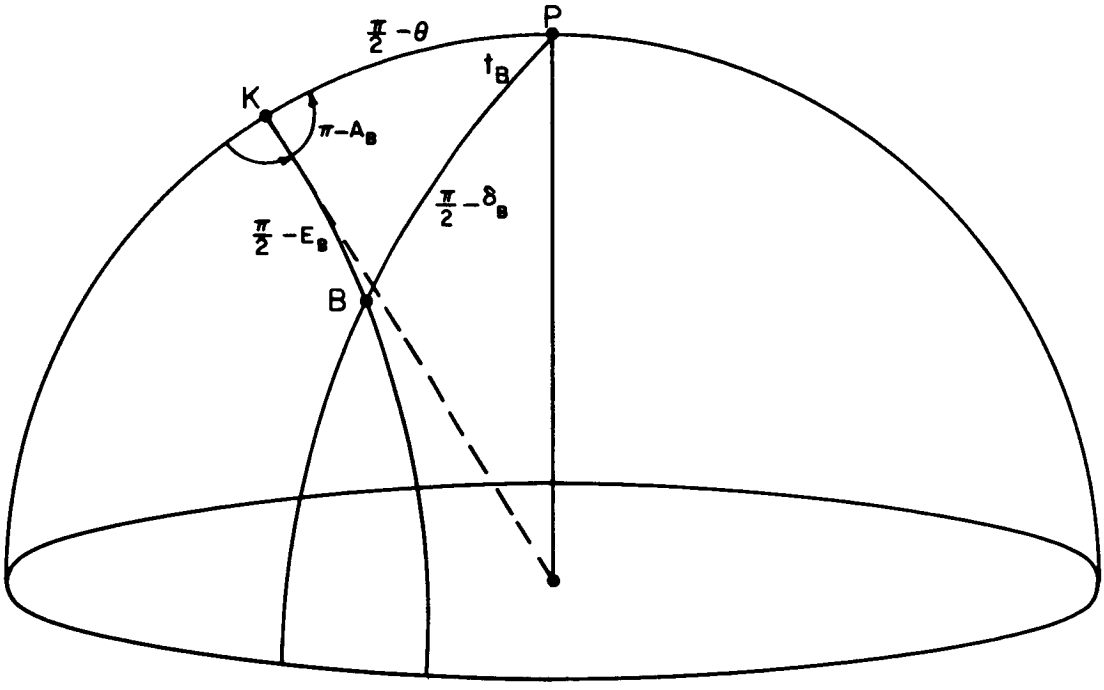

FIGURE 6

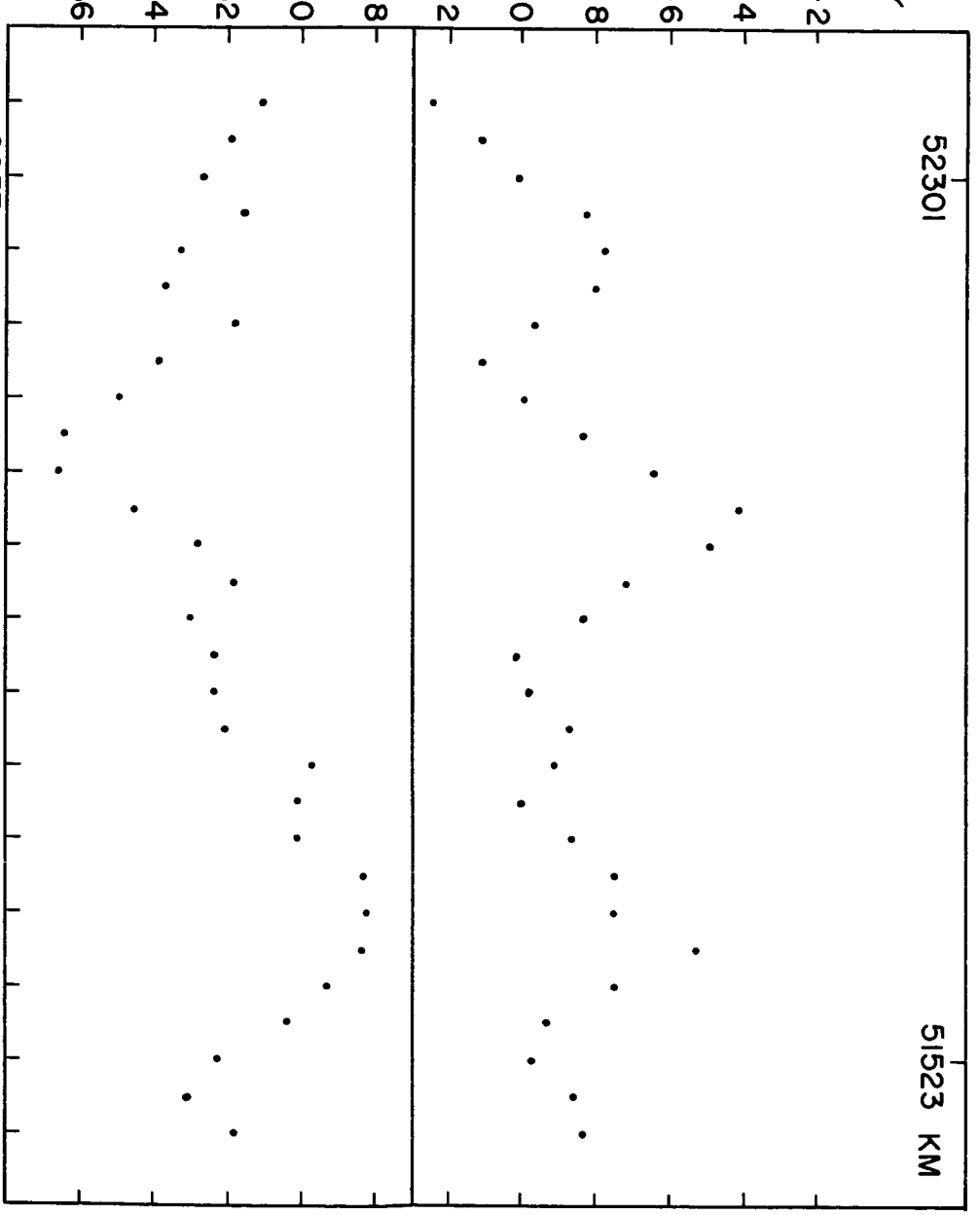
γ
-2
-4
B_r
-6
-8
-10
-12
52301
51523 KM
B_ϕ
-28
-30
-32
-34
-36
2053
2055
2057
2059 UT

FIGURE 7a

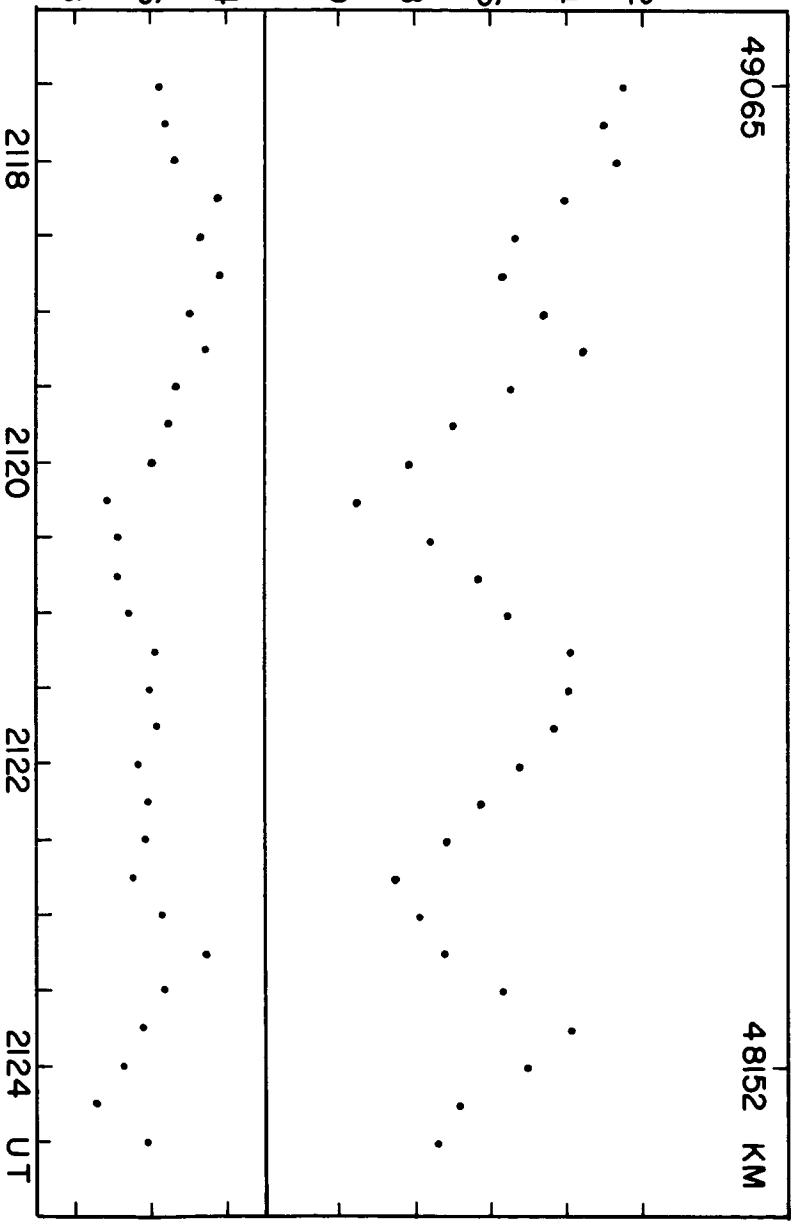

FIGURE 7b

L.T. 1200
λm~+8°

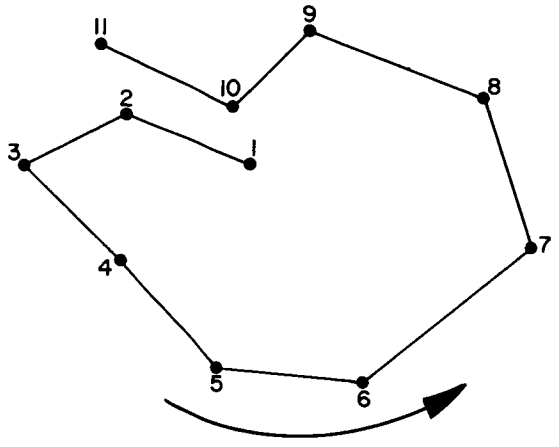

FIGURE 8(1)

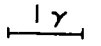

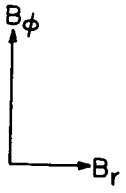

L.T. 1200
λm~+8°

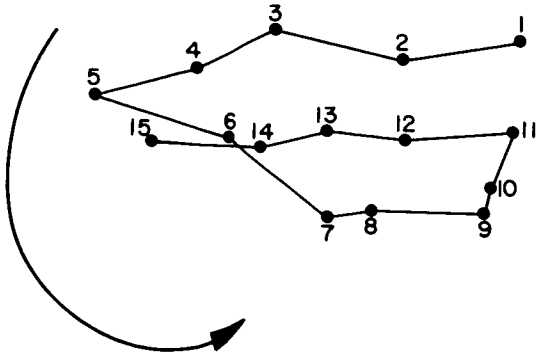

FIGURE 8(2)

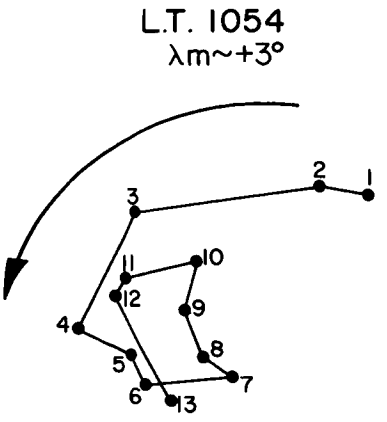

FIGURE 8(3)

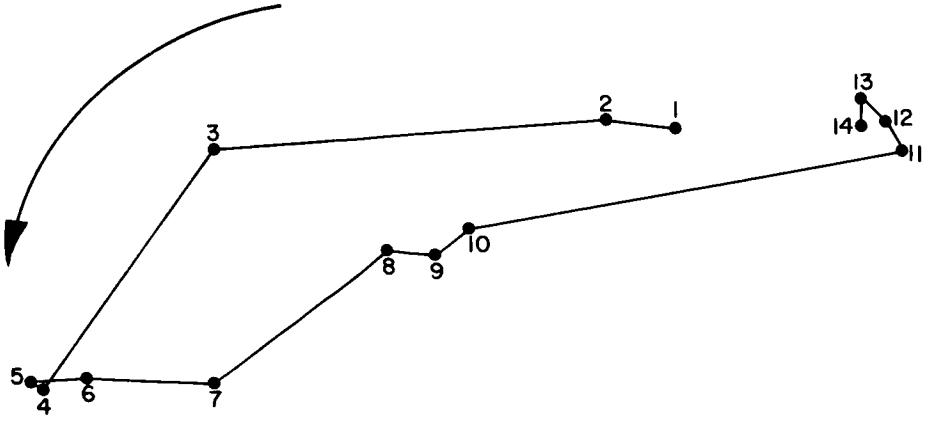

FIGURE 8(4)

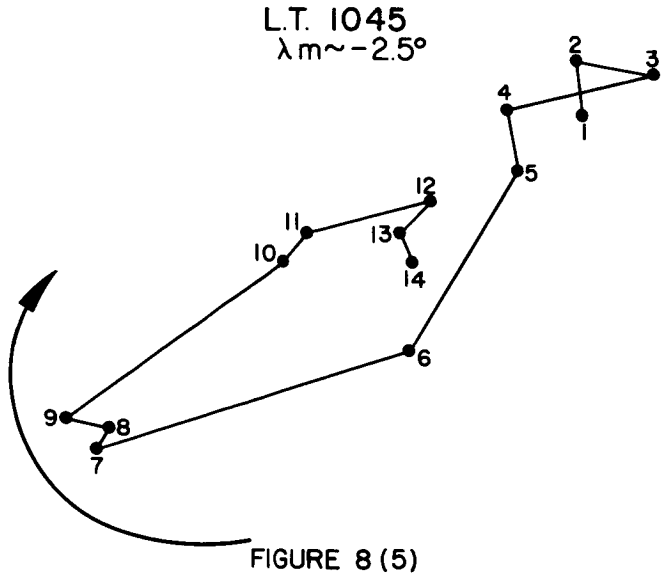

FIGURE 8 (5)

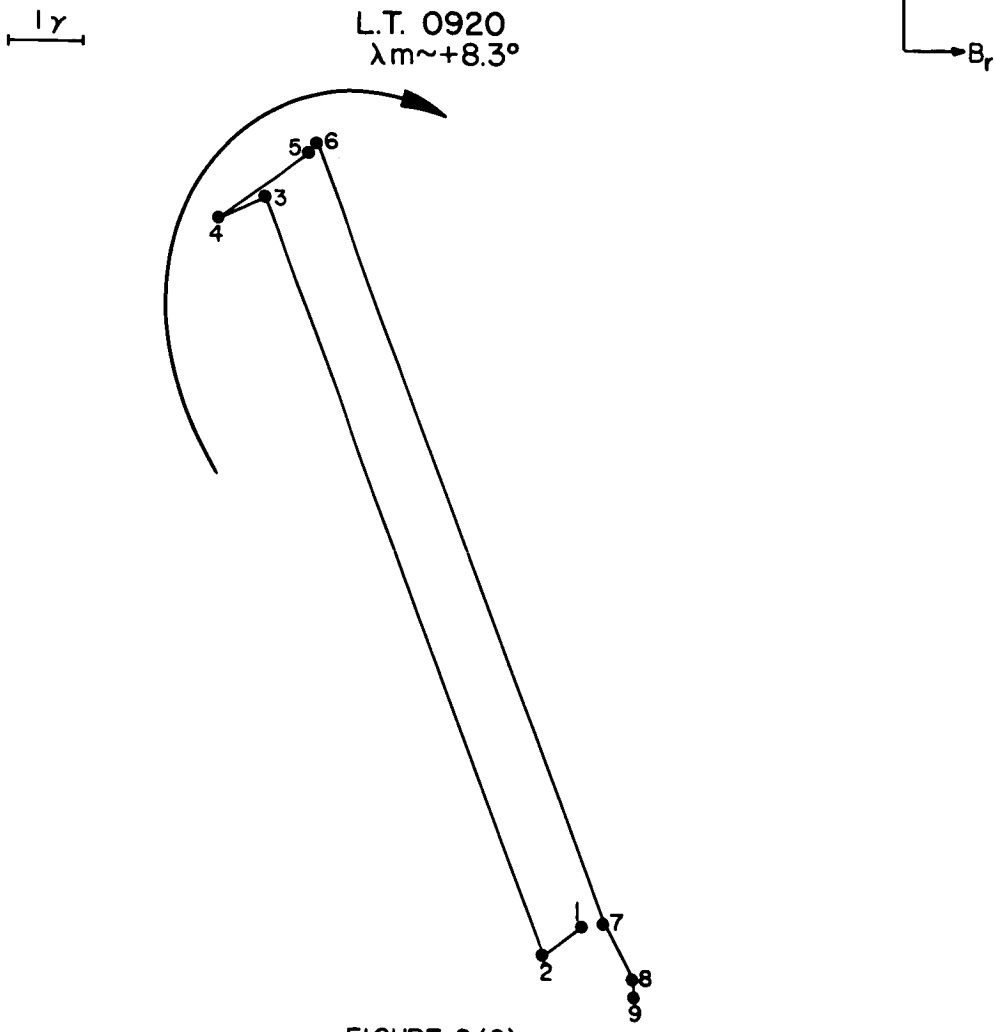

FIGURE 8 (6)

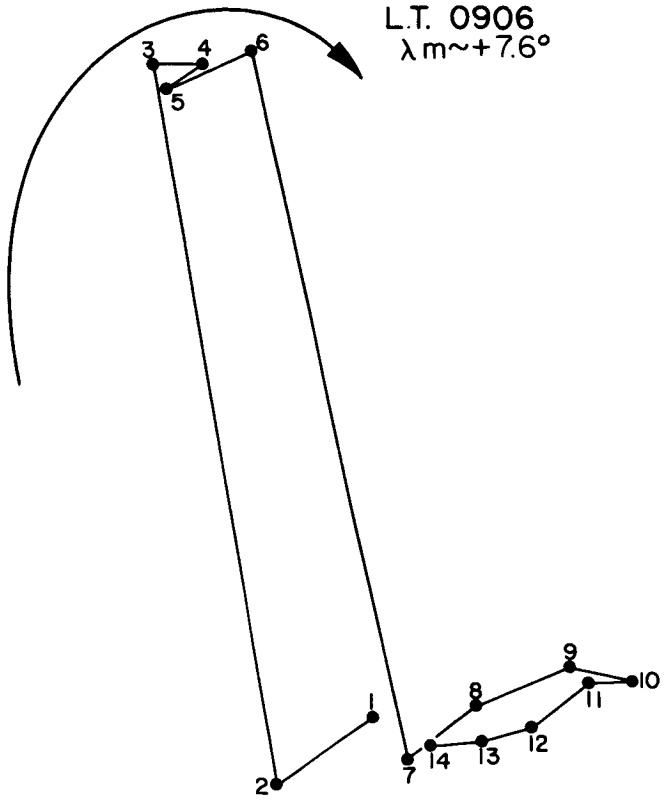

FIGURE 8(7)

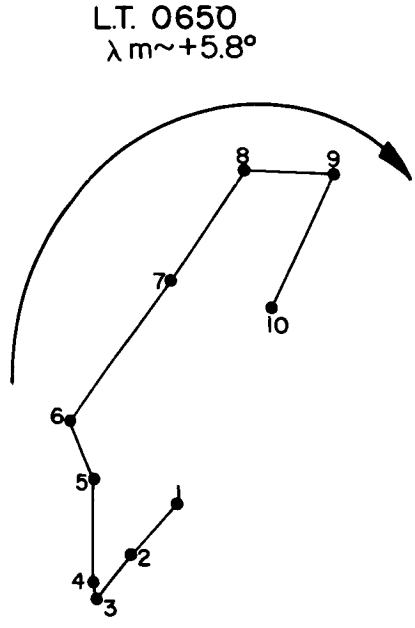

FIGURE 8(8)

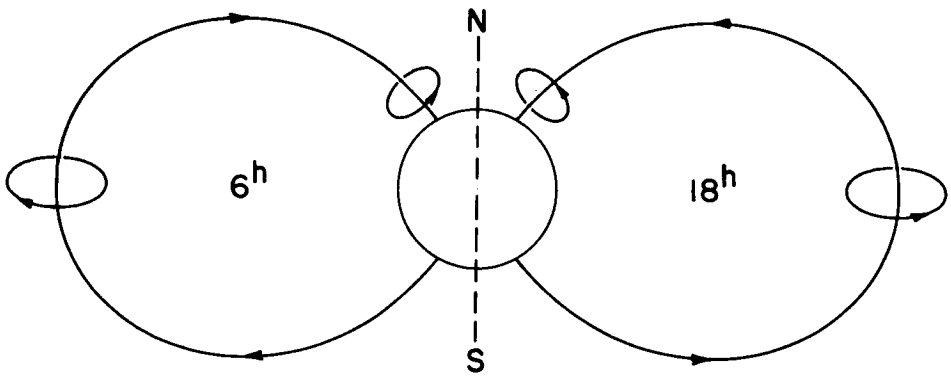

FIGURE 9

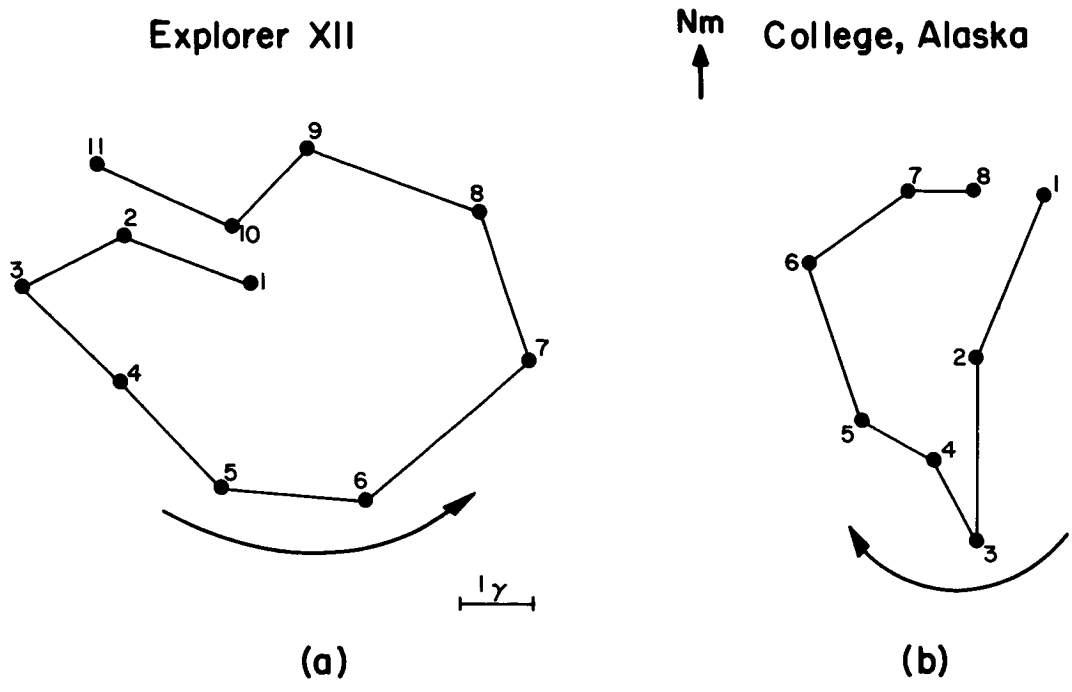
Explorer XII
Nm
College, Alaska
1γ
(a)
(b)

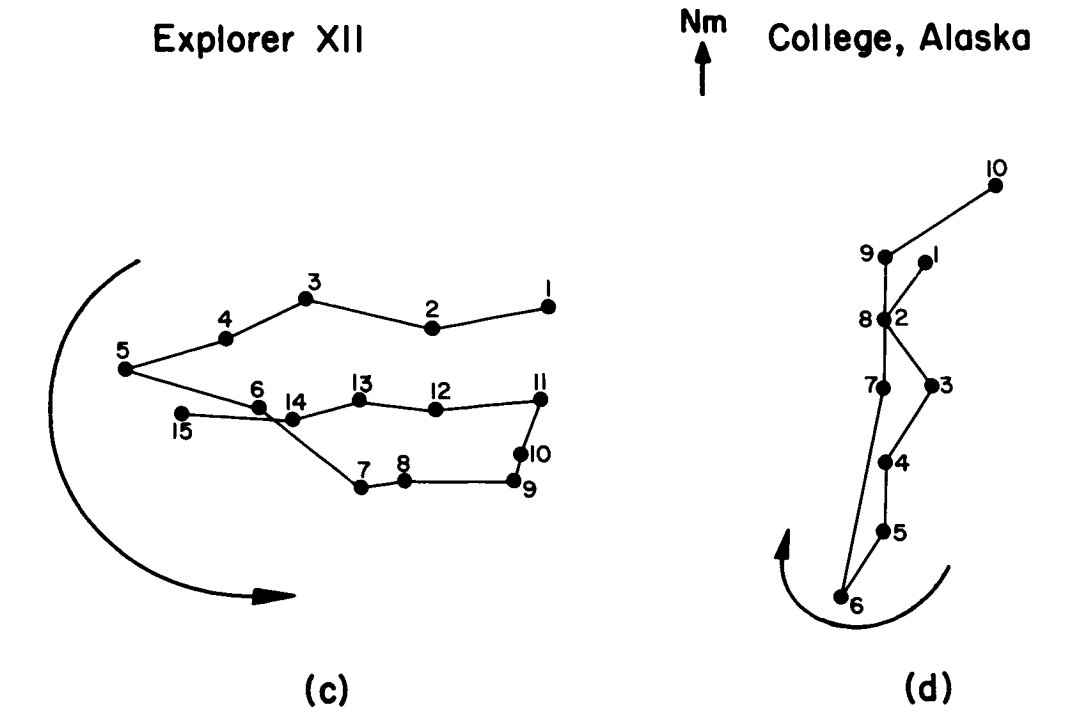
Explorer XII
Nm
College, Alaska
(c)
(d)

FIGURE 10

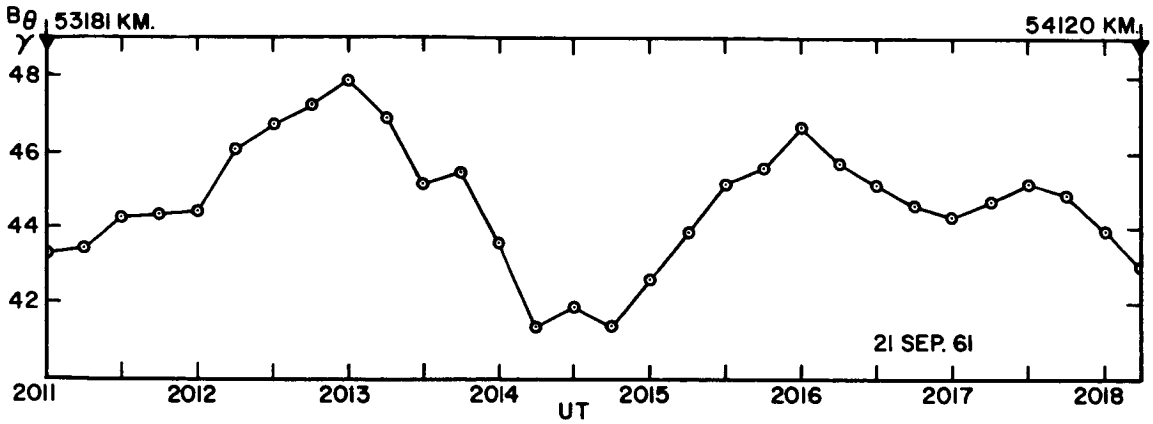

FIGURE 11(1)

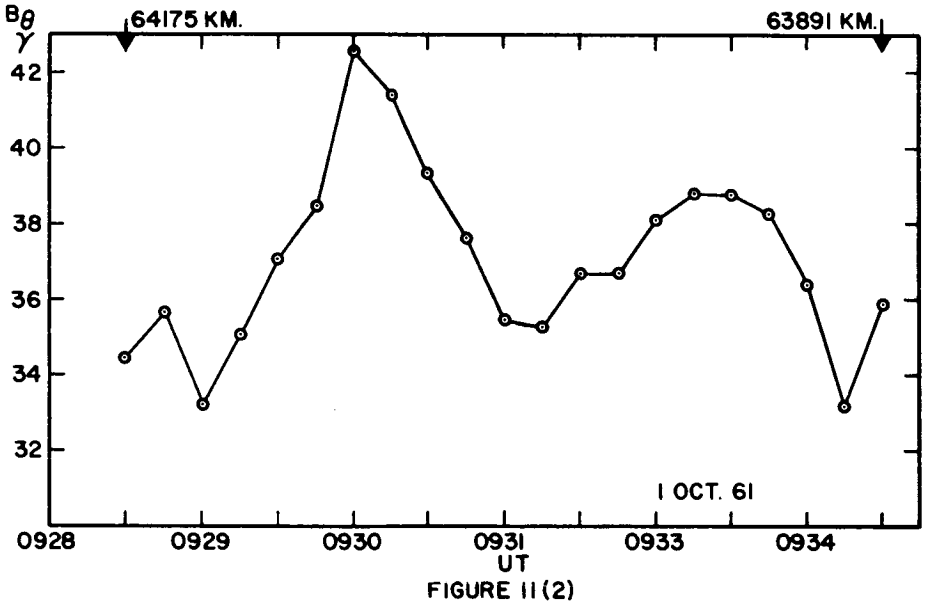

FIGURE 11(2)

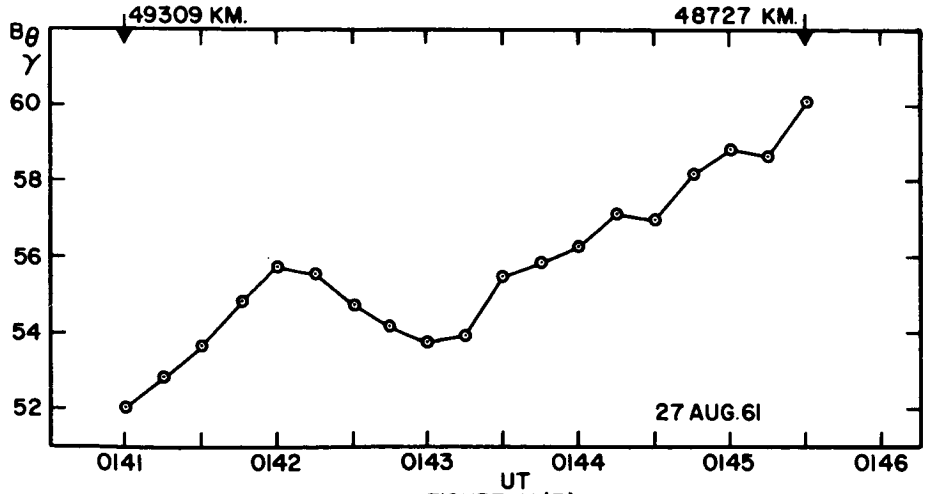

FIGURE 11(3)

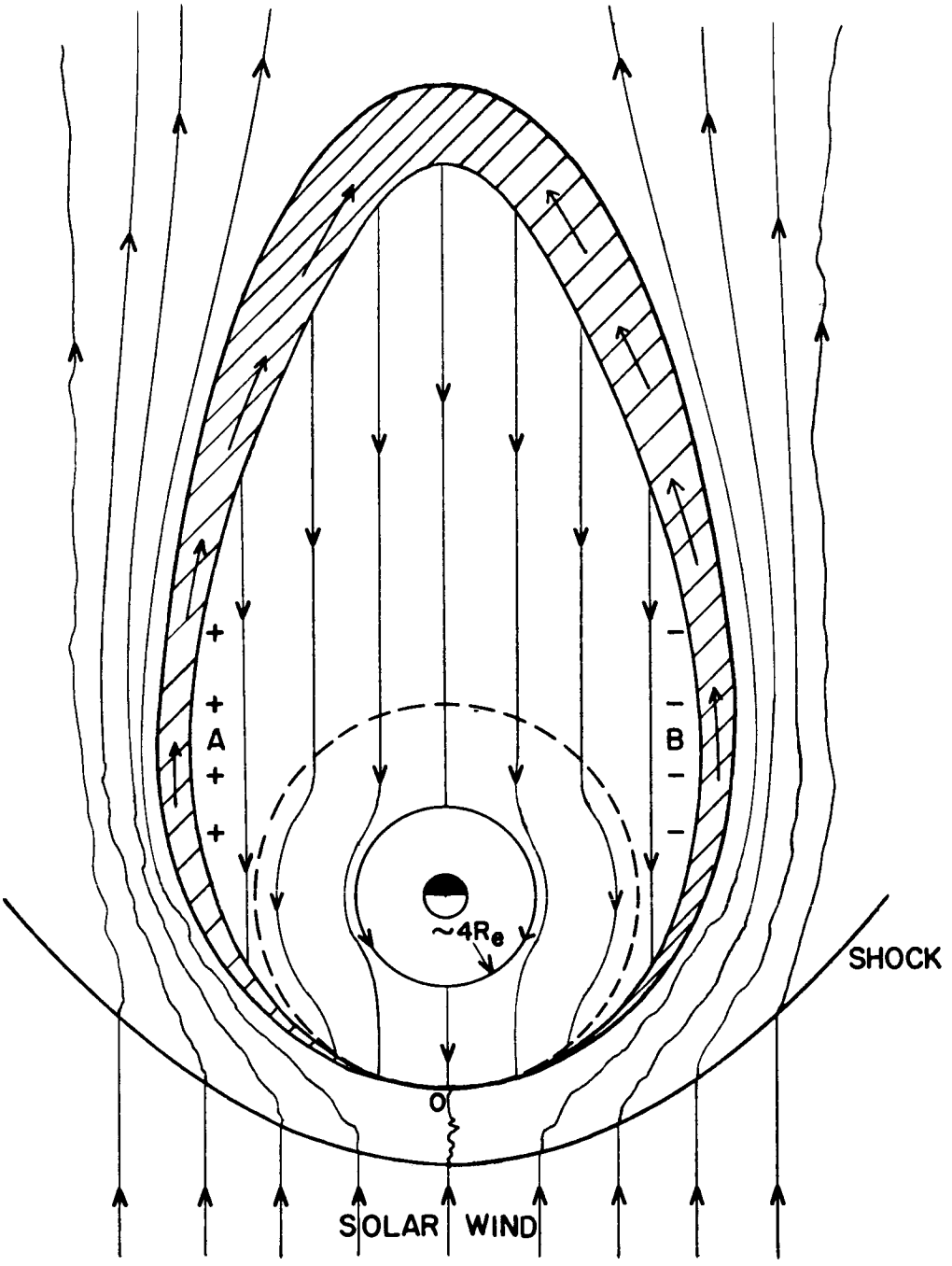

FIGURE 12

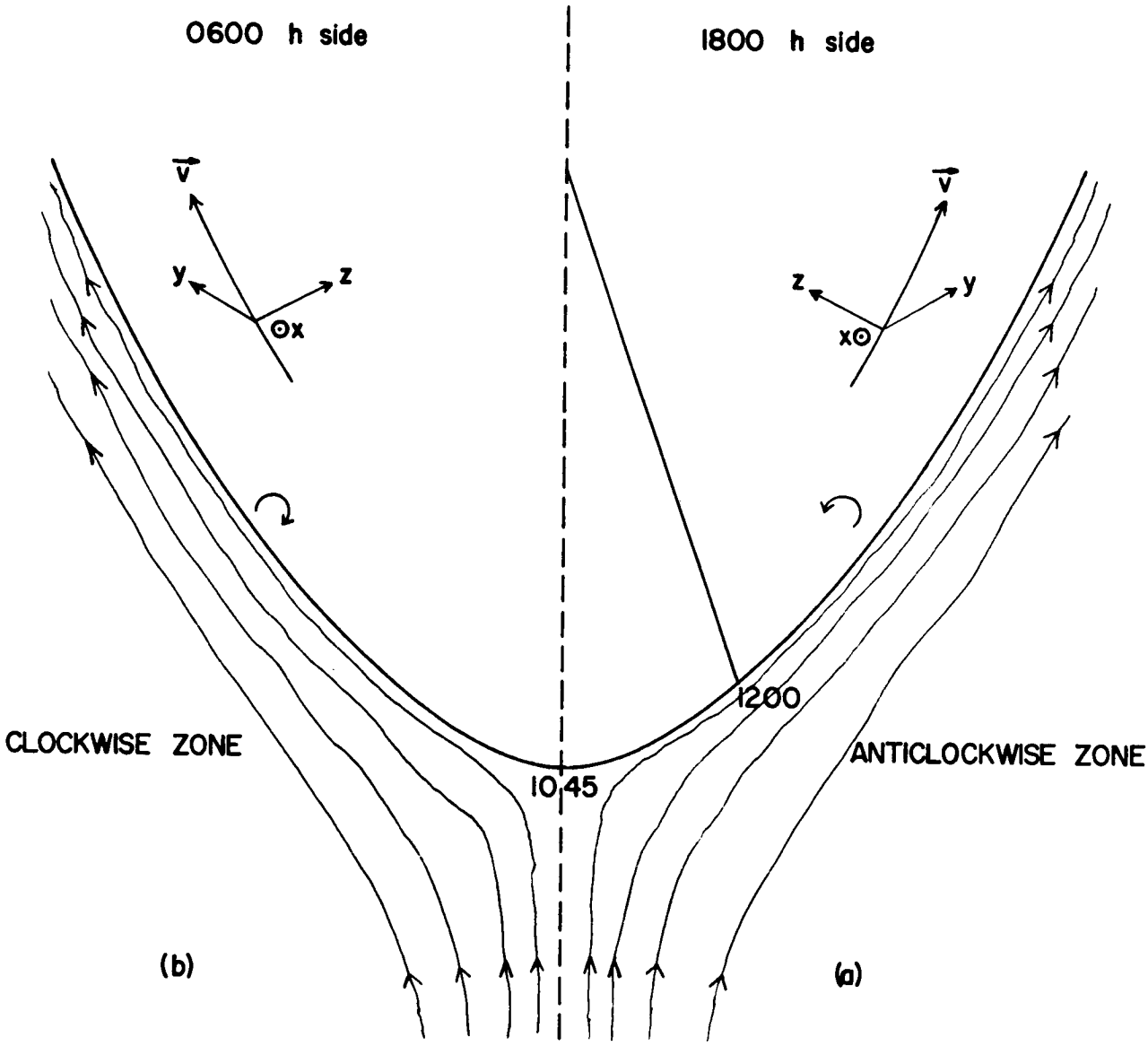
0600 h side
1800 h side
v
y
z
x
v
z
y
x
1200
1045
CLOCKWISE ZONE
ANTICLOCKWISE ZONE
(b)
(a)

FIGURE 13

ERRATA

Page 9	Eqn (4.6) is $\rho_m \frac{d\underline{v}}{dt} = \underline{F}_e + \underline{F}_o$
Page 10	Foot note $\omega << \omega_e$ should be $\omega << \nu_{ei}$
Page 11	Eqn (4.3) J_{conv} should be J_{cond}
Page 11	Line 6 from bottom $\underline{E}$ should be ρE
Page 16	Eqn (7.3) -E should be =E
Page 23	Eqn (2.8) is $\rho = \rho_m$
Page 26	Line 3 is $x^4 + px^2 - q = 0$
Page 36	Line 7 7600 km should be 6700 km
Page 38	Eqn (1.2) B_z should be B_z^2
Page 42	Eqn (3.2) $\underline{J}$ should be J
Page 53	Line 7 (see P.) should be (see P. 34)
Page 57	Line 10 $\pm 3\gamma$ should be 3γ
Page 65	Line 3 from bottom, Satellite[45] should be Satellite[46]
Page 84	Eqn (B.3) add m in denominator on R.H.S.
Page 87	Line 7 'is' should be 'if'
Page 98	Last five lines should be replaced by the following:

"A second problem is a change in the sensitivity or change in slope of the signal voltage versus magnetic field. This problem is easier to correct and to detect in satellite use than the first. These problems have been considered in experiment from which the results discussed in Chapter III were obtained."